Remote Sensing of Environment 194 (2017) 303–321

Contents lists available at ScienceDirect

Remote Sensing of Environment

journal homepage: www.elsevier.com/locate/rse

A nationwide annual characterization of 25 years of forest disturbance and recovery for Canada using Landsat time series

Joanne C. White [a,*], Michael A. Wulder [a], Txomin Hermosilla [b], Nicholas C. Coops [b], Geordie W. Hobart [a]

[a] Canadian Forest Service, (Pacific Forestry Center), Natural Resources Canada, 506 West Burnside Road, Victoria, BC V8Z 1M5, Canada
[b] Department of Forest Resource Management, Forest Sciences Centre, 2424 Main Mall, University of British Columbia, Vancouver, BC V6T 1Z4, Canada

ARTICLE INFO

Article history:
Received 15 September 2016
Received in revised form 14 March 2017
Accepted 28 March 2017
Available online 8 April 2017

Keywords:
Canada
Forest
Monitoring
Landsat
Image processing
Regeneration
Recovery
Disturbance
Wildfire
Harvest

ABSTRACT

In the context of complex demands on forest resources and climate change, synoptic and spatially-explicit baseline data characterizing national trends in forest disturbance and subsequent return of vegetation (and eventual return to forest) are increasingly required. Time series analyses of remotely sensed data enable the retrospective generation of baseline data depicting both forest disturbance and recovery, enabling a more holistic examination of forest dynamics. In this research, we utilize the outputs of the Composite2Change, or C2C, algorithm that leverages the extensive Landsat archive to produce annual, gap-free, surface reflectance composites to date and label disturbance types and to characterize vegetation recovery over the >650 million ha of Canada's forested ecosystems. From 1985 to 2010, 57.5 Mha or 10.75% of Canada's net forested ecosystem area (exclusive of water) were disturbed by either wildfire or harvest, representing an annual rate of disturbance of approximately 0.43% per year. Wildfire accounted for 2.5 times more area disturbed than harvest. On average, wildfire disturbed 1.6 Mha annually and had greater inter-annual variability with a standard deviation of 1.1 Mha, compared to the 0.65 Mha disturbed annually by harvesting ($\sigma = 0.1$ Mha). Herein, we defined a longer-term measure of spectral recovery (the number of years it took for a pixel to attain 80% of its pre-disturbance Normalized Burn Ratio or NBR value), which indicated that harvested areas are recovering more consistently over time relative to areas disturbed by wildfire, with 78.6% of harvested areas requiring ≤10 years to recover, compared to only 35.5% of wildfire areas. A shorter-term (5-year) measure of spectral recovery, also based on the NBR, indicated that vegetation in wildfire areas returned more rapidly than harvested areas; however, when the magnitude of the disturbance was incorporated into the metric, with magnitude typically larger and more variable for wildfire areas, harvested areas were found to be recovering more rapidly on average in the short-term. Overall, <1% of the areas disturbed by wildfire and harvest were identified as non-recovering by all three spectral measures of recovery used in our analysis. Regionally, trends in disturbance and recovery largely echoed trends found at the national level, although the relative amounts and rates of wildfire or harvest varied by ecozone. Time series Landsat composites provide an opportunity to characterize relative trends in disturbance and recovery at a national scale, by disturbance type and ecozone, in a spatially explicit manner and at a level of spatial detail that is relevant to both forest management and science.

1. Introduction

Forest disturbance and recovery represent important ecological processes that strongly impact regional and global forest carbon budgets (Pan et al., 2010; Hicke et al., 2012). Climate change will alter the frequency and intensity of disturbances (Dale et al., 2001), as well as the rate and efficacy of forest regrowth following disturbance (Anderson-Teixeira et al., 2013). In this context of rapid and complex change, baseline information that characterizes historic trends in forest disturbance and recovery over large areas can be valuable reference information for understanding present and future forest dynamics (Cohen et al., 2016). Time series of remotely sensed data, especially Landsat data, offer opportunities to retrospectively generate baseline information on forest disturbance and recovery trends (Frolking et al., 2009) over regions (Kennedy et al., 2012; Griffiths et al., 2014; Potapov et al., 2015), continents (Masek et al., 2008; Lehmann et al., 2012), and the globe (Hansen et al., 2013). The need for this capacity to generate nationally synoptic baseline information is particularly acute in countries such as Canada, which has a large forested area (representing ~10% of global forests), much of which is difficult to access, and where management responsibility is not primarily vested with the federal government, but mainly with multiple provincial and territorial governments and to a lesser extent, private land owners (Wulder et al., 2007).

* Corresponding author.
E-mail address: joanne.white@canada.ca (J.C. White).

http://dx.doi.org/10.1016/j.rse.2017.03.035

Given the disparate jurisdictional responsibilities for forest management in Canada, national datasets summarizing the location and extent of forest disturbances such as wildfire and harvest have historically been compiled from a variety of multi-jurisdictional data sources. For wildfire these national data are spatially explicit (Stocks et al., 2002), but there are no comparable national spatially explicit data for forest harvesting (Masek et al., 2011). Likewise, there are no national or jurisdictional spatially-explicit data sets in Canada that characterize recovery following disturbance. Disturbance monitoring with remotely sensed data has been exhaustively demonstrated (Hansen and Loveland, 2012), and the characterization of post-disturbance recovery has emerged in the applications community (Frolking et al., 2009; Chu and Guo, 2014), enabled by the availability of time series analysis methods and data, particularly Landsat data (Banskota et al., 2014). Remotely sensed data have been used to characterize vegetation regrowth and recovery following wildfire (e.g., Gitas et al., 2012; Chu and Guo, 2014) and less commonly, following harvest (Schroeder et al., 2007; Madoui et al., 2015). Correct attribution of forest disturbance type (i.e., to wildfire or harvest) has important implications for monitoring of recovery for forest management (Schroeder et al., 2011) and carbon accounting (Seedre et al., 2011). Furthermore, recovery trends associated with wildfire and harvesting are expected to vary regionally (Bartels et al., 2016), with implications for the sustainability of management practices and long-term functioning of forest ecosystems.

Unlike wildfire and harvest, which are typically discrete, episodic events (in both space and time), vegetation recovery post disturbance is a process rather than a state, and as such manifests as the initial re-establishment of vegetation at a site through to the full return of forest structural characteristics that were present pre-disturbance (e.g. LePage and Banner, 2014). In the context of this study, and following on the definition of Bartels et al. (2016), we define recovery as the re-establishment and regrowth of vegetation at a site following a stand replacing disturbance, specifically wildfire and harvesting. In an ecological or silvicultural context, this often implies the re-establishment of forests over time, and can be quantified by measurements of canopy cover, height, basal area, and stem density, among others. These measurements are typically acquired via ground measurements (e.g., Bartels et al., 2016), but indicators of recovery, such as vegetation height and density, can also be measured using airborne laser scanning data (e.g., Magnussen and Wulder, 2012; Slesak and Kaebisch, 2016). As noted by others, spectral recovery, as measured with a time series of optical satellite data, is not a direct measure of forest recovery (Kennedy et al., 2012; Griffiths et al., 2014) and must therefore be interpreted in the context of a priori expectations of recovery, which are typically derived from ground plot measurements. However, as demonstrated in Bartels et al. (2016), it is difficult to characterize national trends in post-disturbance recovery for a nation as large and diverse as Canada on the basis of ground plot measurements alone. Thus, information from remotely sensed data can provide a useful framework for assessing relative rates and changes in spectral recovery that provides a national assessment of trends. These trends can be related to available ground observations, and can form the basis for additional sampling and investigations to further relate spectral measures of recovery to ecological and silvicultural understanding of the recovery process (Gómez et al., 2011; Kennedy et al., 2012). Moreover, considering both the depletion (disturbance) and accrual (regrowth) of vegetation provides a more holistic framework for understanding forest change in the context of long-term forest monitoring and carbon accounting.

The objective of the study presented herein was to demonstrate technical capacity and to characterize national trends in stand replacing forest disturbance caused by wildfire and harvest, and subsequent recovery, for the period 1985–2010 for Canada's forested ecosystems (~650 Mha), using information derived from Landsat time series data. Previous studies that have characterized national trends in disturbance and recovery in Canada have either focused on wildfire exclusively and have used substantially coarser spatial resolution remotely sensed data (i.e., Advanced Very High Resolution Radiometer or AVHRR 1- and 8-km data) (Amiro et al., 2000; Hicke et al., 2003; Goetz et al., 2006), or have been sample-based (Frazier et al., 2015; Pickell et al., 2016). Moreover, previous studies that have used Landsat time series data to characterize annual trends in disturbance and recovery have not considered such a large area, nor have they distinguished by disturbance type (Kennedy et al., 2012; Griffiths et al., 2014). In this context, the unique contribution of this work is to use a wall-to-wall time series of Landsat data (with a 30 m spatial resolution) to characterize national spatial and temporal trends in both disturbance and recovery, and to distinguish these trends by disturbance type (wildfire and harvest). By leveraging recent advances in image compositing capability and the holdings of the Landsat archive, we generated a synoptic, consistent national baseline of stand-replacing forest disturbance and recovery and characterized important regional variations in the disturbance and recovery trends observed. These baseline data provide unprecedented reference information against which present and future trends in disturbance and recovery can be assessed.

2. Methods

2.1. Study area

Approaching one billion hectares in area, Canada is a large nation with a gradient in ecosystem productivity that is influenced by latitude and precipitation (Hofgaard et al., 1999). Forested ecosystems represent approximately 65% of Canada's land area (~650 Mha; Wulder et al., 2008). Ecozones represent broadly defined ecological units characterized by "interactive and adjusting abiotic and biotic factors" (Ecological Stratification Working Group, 1996). The Boreal and Taiga Shield ecozones have large west-east extents and are often split into their western and eastern components to reflect differences in ecoclimatic conditions between these regions (Stocks et al., 2002, Frazier et al., 2015). We have likewise split these two ecozones into their western and eastern components (Fig. 1A), resulting in twelve ecozone units for our assessment of national trends in disturbance and recovery.

These ecozones represent a broad range of forest conditions in Canada and may be differentiated by the relative abundance of forests, the productivity and growing conditions in these forests, and the degree of forest management and human population density within the ecozone (Table 1).

Canada's managed forest zone is found primarily in the southern extent of Canada's forested ecosystems (Stinson et al., 2011). These managed forest areas contain forest tenures for harvesting, and also have more intensive fire suppression relative to the unmanaged forest areas. Some ecozones, such as the Atlantic and Pacific Maritime ecozones have 100% of their ecozone area within the managed forest, whereas the Taiga Cordillera has 0% of its area within the managed forest zone. The Boreal Shield East and West have 68% and 62% of their areas, respectively, within the managed forest zone (Table 1). Although the eastern and western components of the Boreal Shield have similar growing season length, the Boreal Shield East is characterized by greater precipitation in the growing season (509 mm) and greater productivity (average 10-year GPP = 0.881 Kg C m^{-2} yr^{-1}), whereas the Boreal Shield West, which is dominated by fire, is notably drier, and receives less precipitation in the growing season (365 mm) and has lower productivity (average 10-year GPP = 0.763 Kg C m^{-2} yr^{-1}) (Table 1).

2.2. Data

2.2.1. Composite2Change (C2C) outputs

Using the Composite2Change or C2C algorithm, annual, cloud-free, Landsat surface reflectance image composites with a 30 m spatial resolution were developed for Canada for 1984 to 2012 using a best-available-pixel (BAP) compositing algorithm (Hermosilla et al., 2016).

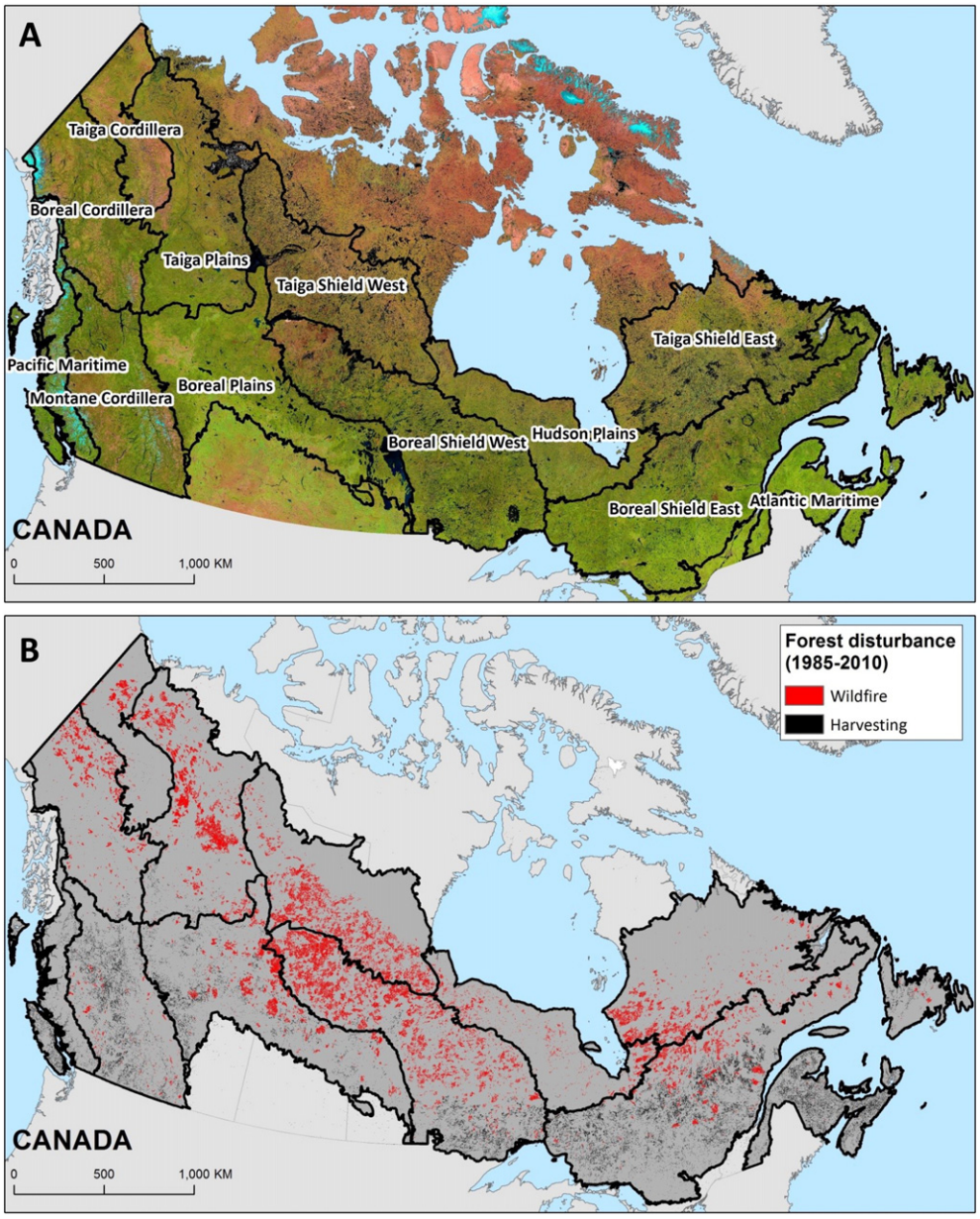

Fig. 1. Best Available Pixel (BAP) proxy image composite of Canada in 2010 (Landsat TM/ETM+ bands 5,4,3) superimposed with the boundaries of the forested ecozones analyzed in this study (A). Area disturbed by wildfire and harvest (1985–2010), as identified using the Composite to Change (C2C) approach (B).

Annual BAP composites were generated using Landsat Thematic Mapper (TM) and Enhanced Thematic Mapper Plus (ETM+) images acquired within ±30 days of August 1, an automated cloud masking algorithm (Fmask; Zhu and Woodcock, 2014), and a set of rules as detailed in White et al. (2014) and further described in Hermosilla et al. (2016). These rules were used to identify the "best" observation for each pixel, in each year; however some data gaps persisted, motivating additional processing.

The annual BAP composites were further processed to remove noise and fill data gaps, as described in Hermosilla et al. (2015a). Briefly, this noise removal process used an annual pixel-level series of normalized burn ratio (NBR; Key and Benson, 2006) values to identify and remove anomalous spectral observations in the temporal domain that may result from undetected clouds, cloud shadows, haze, or smoke. The noise removal process thereby resulted in additional data gaps in the annual BAP composites. The NBR time series for each pixel was also used to identify spectral trends and detect changes in the temporal domain with the breakpoint detection algorithm of Keogh et al. (2001). Change detection in the temporal domain was followed by contextual analysis in the spatial domain, in order to improve the spatial cohesion and uniformity of change events, as described in Hermosilla et al. (2015a). Analysis in the spatial domain also resulted in the removal of changes that are smaller than the defined minimum mapping unit of 0.5 ha. Once changes were identified through the breakpoint detection process, data gaps in the annual BAPs were then infilled with proxy surface reflectance values using the aforementioned spectral trend information and piecewise linear interpolation, applied to each pixel's time series (Hermosilla et al., 2015a). The culmination of this processing were gap-free, surface reflectance proxy image composites at 30 m resolution, annual change detection information, and a series of descriptive change metrics that characterize the change events (i.e., magnitude, duration), as well as the pre- and post-change conditions (Hermosilla et al., 2016).

Detected changes were then attributed to a change type according to the change hierarchy and methods described in Hermosilla et al. (2015b, 2016), with both stand-replacing and non-stand

Table 1
Selected characteristics of Canada's forested ecozones.

ECOZONE	Proportion of net ecozone area that is considered forested (circa 2000)[a]	Proportion of ecozone that is considered managed (%)	GPP 10-year mean GPP (kg C m^{-2} $year^{-1}$)[b]	2006 population density (number of persons per km^2)[c]	Mean growing degree days (1970–2010)[d]	Mean growing season precipitation (mm) (1970–2010)[d]
Atlantic Maritime	82.27	100.00	1.181	12.687	1376	631
Boreal Cordillera	68.75	41.02	0.406	0.068	452	222
Boreal Plains	61.47	87.38	0.845	1.096	1135	324
Boreal Shield East	78.17	68.23	0.881	1.505	1041	509
Boreal Shield West	68.63	61.82	0.763		1097	365
Hudson Plains	57.15	19.55	0.531	0.023	802	340
Montane Cordillera	71.89	100.00	0.630	1.784	674	302
Pacific Maritime	59.33	100.00	0.798	15.418	832	946
Taiga Cordillera	47.20	0.00	0.297	0.002	338	183
Taiga Plains	65.34	17.51	0.512	0.034	794	193
Taiga Shield East	61.45	6.28	0.352	0.030	484	346
Taiga Shield West	45.73	2.07	0.315		606	175

[a] Woodcock et al. (2008).
[b] Zhao et al. (2005).
[c] Statistics Canada (2008).
[d] McKenney et al. (2013).

replacing disturbances being identified. The four change types were wildfire, harvesting, road, and non-stand replacing change. Non-stand replacing changes relate to temporary variations in vegetation condition (Vogelmann et al., 2016) such as defoliating insects, or longer-term gradual changes in vegetation condition (Cohen et al., 2016) such as water stress. Changes were attributed at the object-level using spectral, temporal, and geometrical characteristics of the change objects, and a random forest classifier (Breiman, 2001). Disturbances associated with wildfire and timber harvesting were the most prevalent stand replacing disturbance types and a more detailed description of the national implementation of the methods described above, including further details on the data used in this study is provided in Hermosilla et al. (2016).

The accuracy of the C2C change outputs was evaluated using independent validation data, derived from systematic visual interpretation of the Landsat time series data, similar to the TimeSync approach established by Cohen et al. (2010), and a common approach used in studies that incorporate Landsat time series data (Banskota et al., 2014). Accuracy assessment procedures outlined in Olofsson et al. (2014) were implemented, as detailed in Hermosilla et al. (2015b and 2016). Briefly, this assessment was national in scope and included a stratified random sample of pixels representing both change and no change, and each of the identified change types. Overall change detection accuracy was 89%, with 89.3% of changes labelled to the correct year (97.7% labelled to within ± 1 year) (Hermosilla et al., 2016). User's and producer's accuracies for wildfire were 98% and 93% respectively, and for harvesting, user's and producer's accuracies were both 88%.

2.2.2. Existing national wildfire and harvest data for Canada

Existing information on wildfire and harvesting in Canada varies by jurisdiction and national datasets that are used for reporting purposes are compilations of these jurisdictional sources. There are currently no national, spatially-explicit records for forest harvesting. The Canadian Forest Service maintains the National Forestry Database (NFD; http://nfdp.ccfm.org/), which is a compendium of national forest statistics. The area harvested is reported annually by each jurisdiction in Canada. We downloaded the total area harvested data (1985–2010) for comparison to our C2C harvesting summaries. The NFD data have a few caveats worth noting: in some jurisdictions, harvesting on private land is not reported, but rather is estimated using a volume-to-area conversion factor of 130 m^3/ha; all types of harvesting are reported, including partial or selective harvests; harvesting is sometimes reported from operational plans, which may not represent the actual areas harvested in any given year; and lastly, reporting methods have varied by jurisdiction and over time. Furthermore, the reporting period for government agencies typically is from April 1 of the calendar year to March 31 of the following calendar year, and for years pre-1990, the NFD contains harvest numbers that were estimated by the Canadian Forest Service (i.e., not reported by jurisdictions). Lastly, the NFD reports harvest by jurisdiction, not by ecozone, and while C2C estimates of harvest are restricted to forest dominated ecosystems (Fig. 1A), the NFD includes harvest data from outside this area (which is expected to represent a small area). Given these caveats, differences in total area reported as harvest are expected between the C2C spatial output and the NFD aspatial estimates.

The NFD also reports statistics related to wildfires in Canada's forests. As with the harvest data, this data is aspatial and is reported by jurisdiction, not by ecozone. However, the Canadian Forest Service also maintains the Canadian National Fire Database (CNFDB; http://cwfis.cfs.nrcan.gc.ca/ha/nfdb), which is a spatial database representing wildfire events from 1959 to present day. The CNFDB represents a collection of data compiled from various jurisdictional fire management agencies and from Parks Canada and replaces the former Large Fire Database (Stocks et al., 2002). As noted in the CNFDB metadata, these data are not considered exhaustive or without error, with data accuracy varying by source agency, year, and the different mapping techniques used to capture the fire perimeters (e.g. manual delineation on base maps, air photos, airborne GPS surveys, satellite data; Canadian Forest Service, 2015). Mapping methods have varied through time, with improvements in automation, spatial accuracy, and precision resulting from the increased use of GPS, GIS, and satellite data in the last decade. While the location of the fires is generally regarded as accurate, information on the size and perimeter of the fires is in some cases unknown, and in other cases may be poorly mapped. As a result, the frequency of fire events is expected to be more accurate than the actual size of the area burned or the shape of the fire perimeter. For example, unburned islands and water bodies within fires are typically not excluded from the fire perimeter and may contribute to an overestimation of area disturbed by wildfire (Parisien et al., 2006).

2.3. Characterizing vegetation recovery

While numerous approaches have been used to characterize post-disturbance recovery, vegetation indices and derivatives thereof have been the most common (Chu and Guo, 2014) and the Normalized Difference Vegetation Index (NDVI) has been the predominant spectral index for evaluating post-fire recovery (e.g., Gitas et al., 2012; Veraverbeke et al., 2012a and 2012b; Vila and Barbosa, 2010). Given the profusion of indices and metrics available for assessing post-disturbance vegetation recovery, the work of

Pickell et al. (2016) has helped to clarify the relative strengths of commonly used indices including NDVI, NBR, Tasseled Cap Greenness (TCG), and the shortwave-infrared band (SWIR; Landsat TM/ETM+ band 5). While NDVI and TCG can characterize the initial pulse of vegetation that establishes at a site post-disturbance, these indices saturate rapidly (e.g., Buma, 2012; Chu et al., 2016) and therefore provide little indication of the progression of the recovery process over time. In contrast, indices such as NBR, which incorporate the shortwave infrared (SWIR) wavelength, are more strongly linked to vegetation structure and therefore are expected to provide an indication of the increasing forest structural complexity commonly associated with forest regeneration (Frazier et al., 2015; Ireland and Petropoulos, 2015). Horler and Ahern (1986) identified the importance of the shortwave-infrared wavelengths for characterizing forest structure, particularly for regenerating stands.

The importance and utility of the short-wave infrared (SWIR) wavelengths for characterizing forest structure is well understood (Cohen and Goward, 2004), and has been demonstrated in the context of forest recovery following disturbance (Epting and Verbyla, 2005; Pflugmacher et al., 2014). Wulder et al. (2009) found that post-fire forest structural conditions measured from LiDAR were strongly correlated with the NBR (Key and Benson, 2006). Kennedy et al. (2010) found the NBR to be the most sensitive spectral index for capturing disturbance events from Landsat time series data and is the spectral index deployed in the LandTrendr algorithm (cf. Meigs et al., 2011; Kennedy et al., 2012) and the C2C algorithm (Hermosilla et al., 2016) used to generate the data used in this study. Cohen et al. (2010) tested and found comparable performance between the NBR and tasseled cap wetness (TCW) for detecting disturbance and recovery: NBR was more sensitive to disturbance than TCW, whereas TCW underestimated recovery.

One objective of this study was to characterize national spatial and temporal patterns in post-disturbance vegetation recovery. Herein, we define recovery as being both the initial establishment (or pulse of vegetation), as well as a more long-term, sustained regeneration of forests at a site (Johnstone et al., 2004). Therefore, we have used metrics that allow us to characterize both shorter- and longer-term aspects of vegetation recovery. Pickell et al. (2016) found that different spectral indices measure different aspects of recovery, which was further demonstrated in the work of Chu et al. (2016), who proposed the use of different indices to characterize shorter- and longer-term recovery in Siberian larch forests. We used the NBR to derive our recovery metrics; the NBR is a spectral index that was first introduced by Key and Benson (2006) to map burn severity, and is calculated using Landsat TM/ETM+ bands 4 (B4; near-infrared) and 7 (B7; shortwave-infrared), as follows:

$$\mathrm{NBR} = \frac{\mathrm{B4}-\mathrm{B7}}{\mathrm{B4}+\mathrm{B7}} \quad (1)$$

The NBR was designed to take advantage of the different spectral responses that disturbed and undisturbed areas will have in these two spectral regions. NBR values range from −1 to 1, with positive values for pixels dominated by vegetation, and negative values for pixels dominated by bare soil (Escuin et al., 2008). Our recovery metrics are developed using trend-fitted NBR values from our time-series analysis (i.e., from the proxy surface reflectance BAP composites described in Section 2.2.1), to which we applied a despiking approach similar to that of Kennedy et al. (2010) and Bolton et al. (2015), where noisy observations are detected by examining them in relation to their previous and subsequent spectral values in the time series (Hermosilla et al., 2015a). As noted by Schroeder et al. (2007), year-to-year differences that result from phenology or atmospheric effects such as haze will be minimized by a fitted trajectory curve.

Our first metric was an absolute measure of post-disturbance regrowth, which is considered as a spectral proxy for recovery (Griffiths et al., 2014). As defined by Kennedy et al. (2012), this metric indicates the change in NBR at five years following disturbance:

$$\Delta\mathrm{NBR}_{\mathrm{regrowth}} = \mathrm{NBR}_{\mathrm{fitted,y5}} - \mathrm{NBR}_{\mathrm{fitted,y}} \quad (2)$$

where $\mathrm{NBR}_{\mathrm{fitted,y5}}$ is the fitted NBR value 5-years post-disturbance and $\mathrm{NBR}_{\mathrm{fitted,y}}$ is the fitted NBR value in the year of disturbance. Effectively, this metric indicates how much the NBR value for a given pixel has changed over the 5-year period following disturbance.

Our second metric is a relative measure of post-disturbance regrowth. Previous studies have demonstrated the importance of conditioning spectral measures of vegetation recovery on pre-disturbance characteristics (Bolton et al., 2015; Devries et al., 2015; Pickell et al., 2016); and we therefore also included a relative measure of vegetation recovery. Kennedy et al. (2012) defined the Recovery Indicator (RI), which scaled the post-disturbance regrowth ($\Delta\mathrm{NBR}_{\mathrm{regrowth}}$) metric by the magnitude of the disturbance segment:

$$\mathrm{RI} = \frac{\Delta\mathrm{NBR}_{\mathrm{regrowth}}}{\Delta\mathrm{NBR}_{\mathrm{disturbance}}} \quad (3)$$

where $\Delta\mathrm{NBR}_{\mathrm{regrowth}}$ is defined in Eq. (2) and $\Delta\mathrm{NBR}_{\mathrm{disturbance}}$ is defined in Eq. (4) below. While Kennedy et al. (2012) defined magnitude as a percent change in vegetative cover, with NBR values calibrated to cover estimates, herein we have adapted the Recovery Indicator, defining the denominator, $\Delta\mathrm{NBR}_{\mathrm{disturbance}}$, as the change in NBR during the disturbance segment (Fig. 2):

$$\Delta\mathrm{NBR}_{\mathrm{disturbance}} = \mathrm{NBR}_{\mathrm{y}-1} - \mathrm{NBR}_{\mathrm{y}} \quad (4)$$

where $\mathrm{NBR}_{\mathrm{y-1}}$ is the NBR value at the beginning of the disturbance segment and $\mathrm{NBR}_{\mathrm{y}}$ is the NBR value at the end of the disturbance segment. By scaling $\Delta\mathrm{NBR}_{\mathrm{regrowth}}$ by change magnitude, we account for vegetated areas with lower NBR at the time of disturbance, and for lower magnitude disturbances, which may leave more residual vegetation (Kennedy et al., 2012).

Finally, to characterize longer-term aspects of recovery, in our third metric we adapted the approach of Pickell et al. (2016) and determined the length of time it took, in years, for a given pixel to reach 80% of its pre-disturbance NBR value (Years to Recovery or Y2R). The pre-disturbance NBR value was defined as the average NBR value of the two years prior to the disturbance segment, calculated as follows:

$$\mathrm{NBR}_{\mathrm{pre\text{-}disturbance}} = \frac{\mathrm{NBR}_{\mathrm{y}-2} + \mathrm{NBR}_{\mathrm{y}-1}}{2} \quad (5)$$

In the context of our definition of recovery, and given the emphasis that we place on characterizing relative rates of recovery, meeting or exceeding 80% of the pre-disturbance NBR value relates a positive trend in the return of vegetation, but does not necessarily indicate a return to the same forest conditions that existed at a site prior to disturbance. Lastly, to assess recovery, and account for the need to have a 5-year period to generate the $\Delta\mathrm{NBR}_{\mathrm{regrowth}}$ and RI metrics, we included only those pixels disturbed between 1985 and 2005, which represented approximately 85% of all disturbed pixels for 1985–2010.

3. Results

3.1. Disturbance by wildfire and harvest in Canada's forested ecosystems (1985–2010)

From 1985 to 2010, >57 Mha or approximately 10.75% of Canada's net forested ecosystem area (excluding water) were disturbed by wildfire and harvest (Table 2; Fig. 1B; Fig. 3). Nationally, the mean

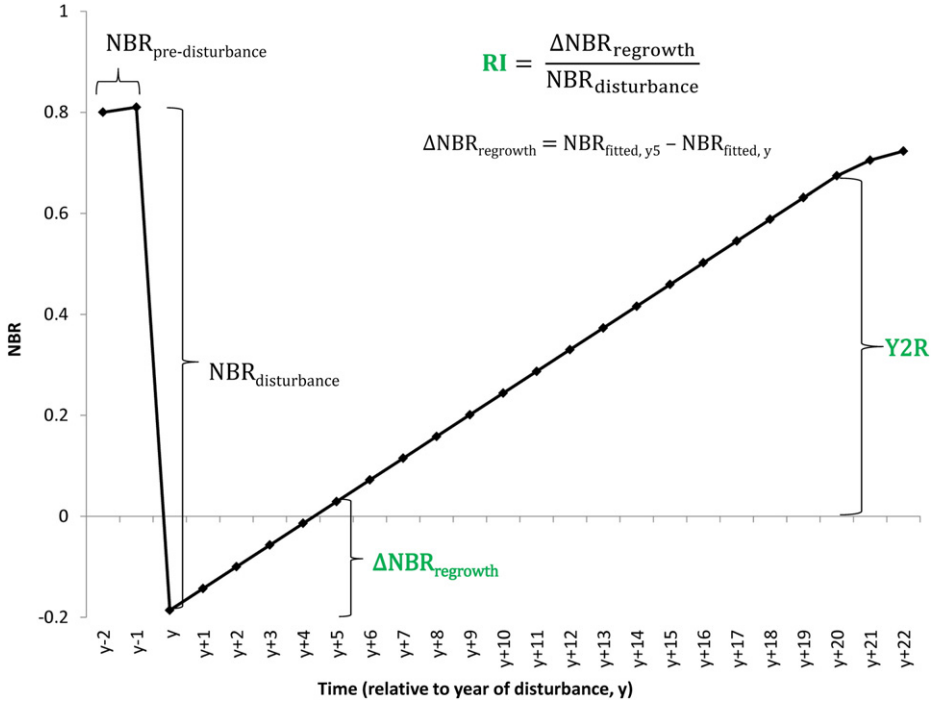

Fig. 2. Schematic of Normalized Burn Ratio (NBR) recovery metrics: $\Delta NBR_{regrowth}$, Recovery Indicator (RI), and Years to Recovery (Y2R).

annual area disturbed is approximately 0.43% per year, with wildfire accounting for nearly 2.5 times as much area disturbed as harvesting (Electronic Supplement Table S1). The amount of disturbance for wildfire and harvesting varies by ecozone, with the largest area of stand-replacing disturbance found in the Boreal Shield West, and the smallest in the Pacific Maritime ecozone (Table 2). Relative to net ecozone area, the Atlantic Maritime ecozone had the largest proportion of area disturbed by harvesting, while the Boreal Shield West and the Taiga Shield West had the largest proportion of area disturbed by wildfire (Fig. 4). The total area disturbed in each ecozone, by year, is summarized in Table S2 (Electronic Supplement). The cumulative net ecozone area disturbed annually, as well as the rate of disturbance by both wildfire and harvest within each ecozone, is summarized in Fig. 5A and B, respectively. The relative contribution of each ecozone to the national total area disturbed by wildfire and harvest is summarized in Table 3.

In the majority of forested ecozones in Canada, the predominant stand replacing disturbance is wildfire. Moreover, for six forested ecozones in particular, wildfire accounted for >95% of the area disturbed in each of these ecozones: Taiga Shield West and East, Taiga Cordillera, Hudson Plains, Taiga Plains, and Boreal Cordillera. Of note, wildfires in these six ecozones alone account for almost 60% of the total area disturbed in Canada's forested ecosystems between 1985 and 2010 (Table 3). In only four of the forested ecozones examined was harvesting the dominant stand-replacing disturbance: Atlantic Maritime, Pacific Maritime, Montane Cordillera, and Boreal Shield East. Harvesting in these four ecozones accounted for 22% of the national area disturbed (1985–2010). In the Atlantic and Pacific Maritime ecozones, harvesting accounted for >97% of the disturbance in each of those ecozones.

More than 40.6 Mha of Canada's forested ecosystems were disturbed by wildfire from 1985 to 2010, with a national average of 1.6 Mha per year. Annual variability in the amount of area disturbed by wildfire ($\sigma = 1.1$ Mha for wildfire) was markedly greater than the annual variability in the area disturbed by harvest ($\sigma = 0.1$ Mha). Temporally, 1995 was the year with the largest area disturbed by wildfire (5.9 Mha), followed by 1989 with 3.5 Mha; combined, these two years account for 23% of the total area burned between 1985 and 2010 (Fig. 3). The years with the least amount of area disturbed by wildfire were 1988 and 2000, with each of these years having <0.6 Mha of wildfire. The Boreal Shield West ecozone had the largest total area disturbed by wildfire from 1985 to 2010 (10.9 Mha), followed by the Taiga Shield West

Table 2
Total area disturbed (ha) by wildfire and harvest in Canada's forested ecozones (1985–2010).

ECOZONE	Total ecozone area (ha)	Net ecozone area (ha) (exclusive of surface water)	Total area disturbed (ha)		
			Wildfire	Harvest	Total
Atlantic Maritime	20,436,453	17,498,799	26,829	2,676,189	2,703,018
Boreal Cordillera	44,469,737	41,090,604	2,554,220	76,745	2,630,965
Boreal Plains	71,318,202	52,500,661	3,388,467	1,965,436	5,353,903
Boreal Shield East	107,710,345	90,912,105	3,521,121	6,341,561	9,862,682
Boreal Shield West	81,817,371	64,301,119	10,908,564	1,784,288	12,692,852
Hudson Plains	36,408,956	33,787,154	1,862,778	31,692	1,894,470
Montane Cordillera	47,786,295	43,306,283	599,529	2,918,129	3,517,658
Pacific Maritime	20,129,744	18,046,293	22,890	852,920	875,810
Taiga Cordillera	25,124,723	23,368,911	993,805	14,969	1,008,774
Taiga Plains	61,991,369	51,945,012	6,139,831	183,901	6,323,732
Taiga Shield East	72,981,422	55,912,847	3,788,123	6825	3,794,948
Taiga Shield West	59,806,905	41,640,865	6,821,715	4202	6,825,917
TOTAL	649,981,522	534,310,653	40,627,872	16,856,857	57,484,729

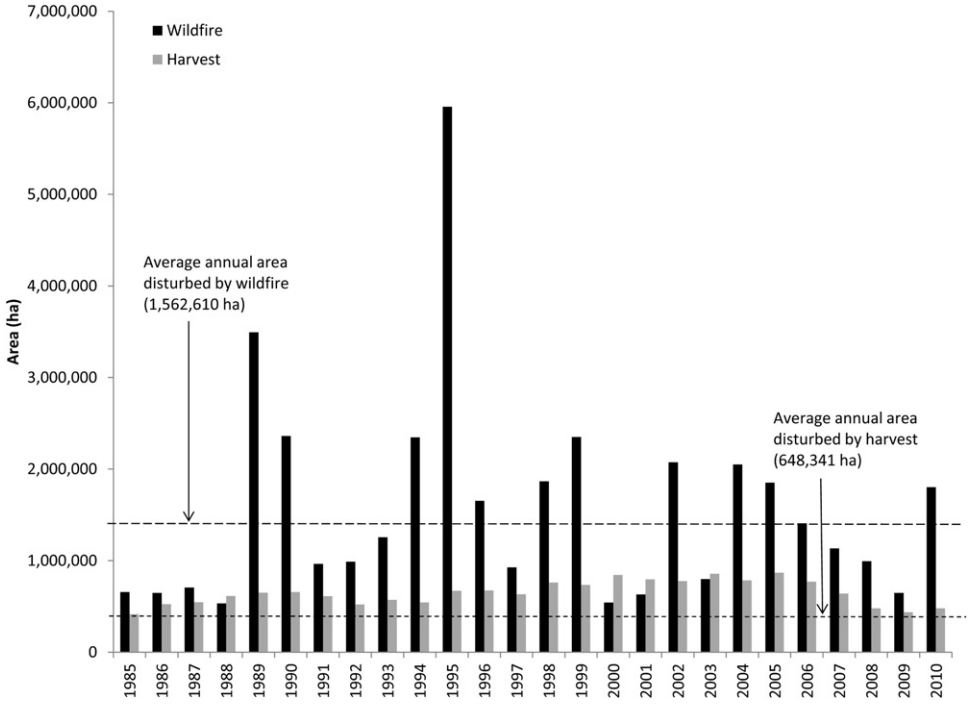

Fig. 3. Annual area disturbed by wildfire and harvest in Canada's forested ecosystems (1985–2010).

(6.8 Mha), while the Atlantic and Pacific Maritime ecozones each had <0.03 Mha of wildfire 1985–2010 (Table 2).

The total area of Canada's forested ecosystems disturbed by harvesting from 1985 to 2010 was 16.8 Mha, with an annual average of 0.65 Mha ($\sigma = 0.1$ Mha) (Table 2, Fig. 3). Temporally the annual area harvested has not fluctuated greatly, with 2005 having the largest area harvested (0.9 Mha) and 1985 having the smallest area harvested (0.4 Mha). The area disturbed by harvesting exceeded the area disturbed by wildfire in only four years: 1988, 2000, 2001, and 2003. The Boreal Shield East ecozone had the largest total area of harvesting (6.3 Mha), followed by the Montane Cordillera (2.9 Mha), and the Atlantic Maritime (2.7 Mha) ecozones (Table 2). The Atlantic Maritime had the largest proportion of its net ecozone area disturbed by harvesting (15.4%), in contrast to that of the Boreal Shield East (6.9%; Fig. 4). Harvesting rates were relatively consistent over time (Fig. 5B), with annual variability in area disturbed by harvest greatest for the Atlantic Maritime ecozone (Table 2).

3.2. Comparison to existing national disturbance data for Canada

We compared the C2C outcomes to existing national data to evaluate whether temporal trends in area disturbed by wildfire and harvest were

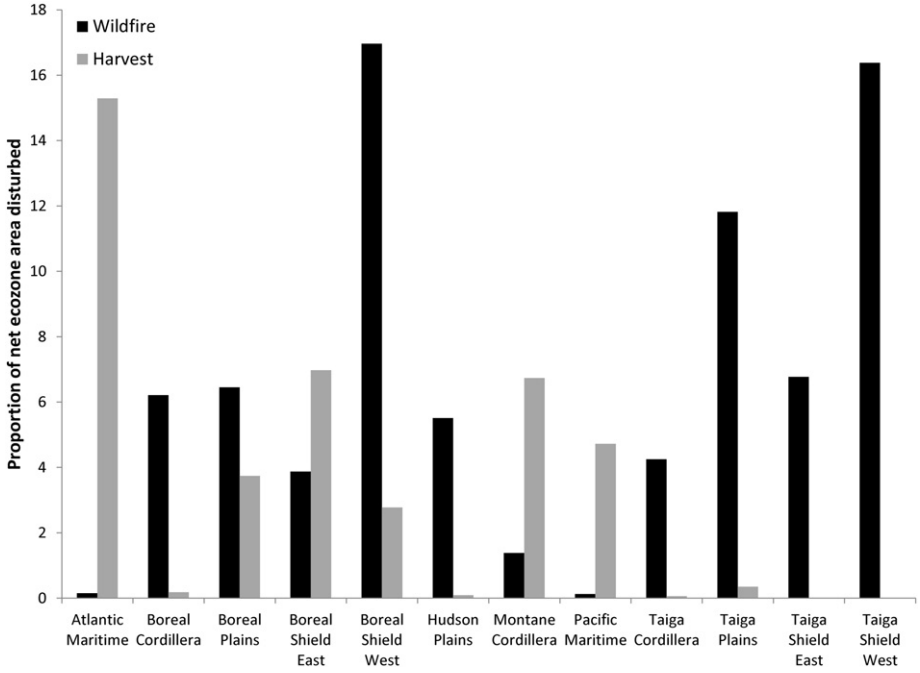

Fig. 4. Proportion of net ecozone area disturbed by wildfire or harvest (1985–2010).

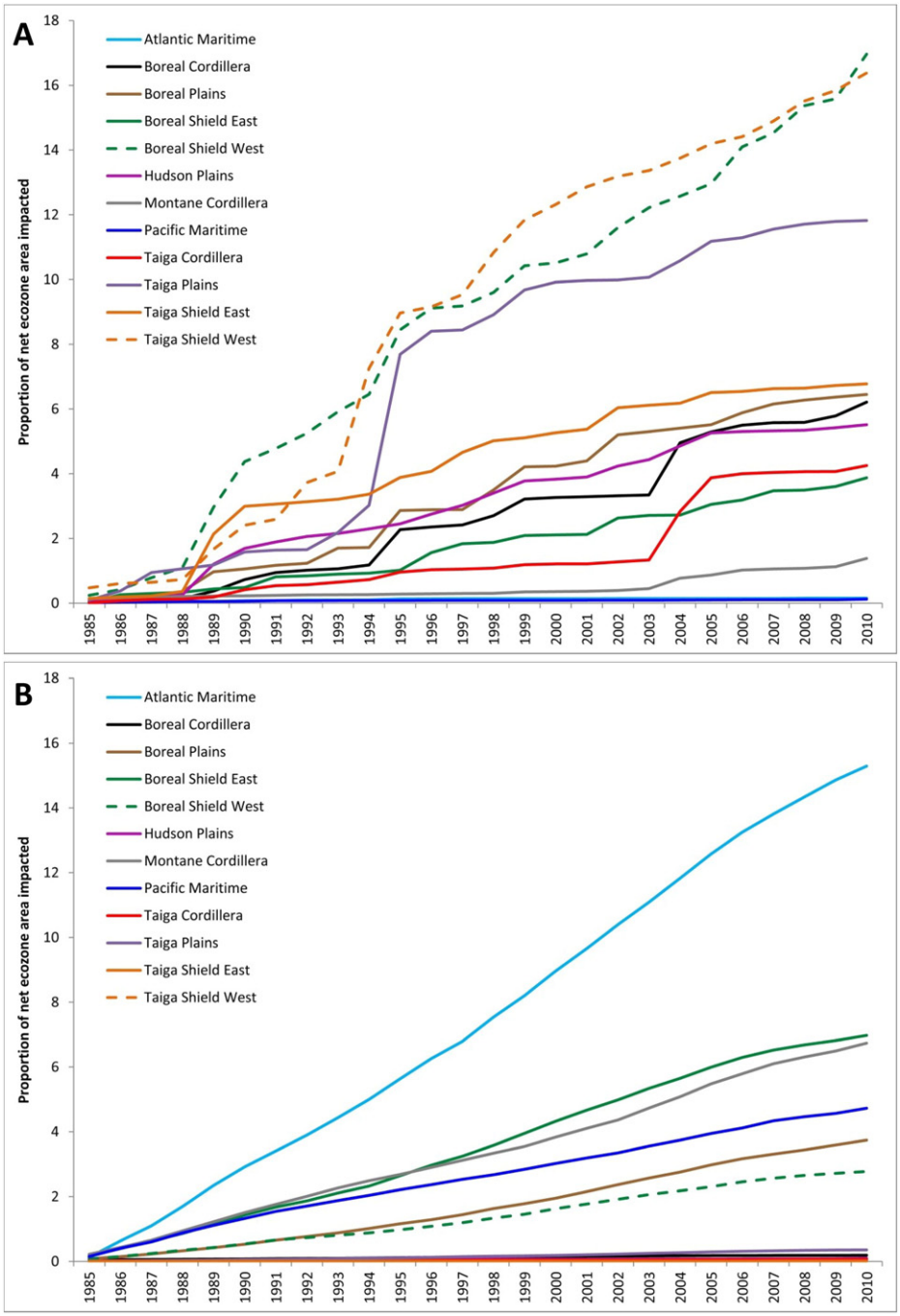

Fig. 5. Cumulative proportion of net ecozone area disturbed by wildfire (A) and harvesting (B) annually from 1985 to 2010. The slope of the cumulative proportion indicates the rate of disturbance.

consistent among the various data sources. Fig. 6 summarizes the comparison between the aspatial NFD and the spatial C2C estimates of harvest area, by year. The average annual area harvested for 1985–2010, as reported by the NFD, was 0.95 Mha (with 0.82 Mha clearcut) compared to the C2C estimate of 0.65 Mha. Trends for total area disturbed by harvest are similar between the NFD and C2C, with area estimates becoming increasingly similar over time.

Fig. 7 summarizes the three-way comparison between the NFD (aspatial), the CNFDB (spatial), and the C2C estimates of total annual area disturbed by wildfire. As per harvest, the temporal trends in area disturbed by wildfire are similar. The NFD and CNFDB both estimate the average annual area disturbed by wildfire at approximately 2.3 Mha, while the C2C estimate is 1.6 Mha. A specific, spatial example of differences between the C2C fire and the CNFDB fire is shown in Fig. 8. The second largest fire in 1989 was located in northwestern Quebec, near Hudson Bay, and had an area of approximately 412,000 ha in the CNFDB. In the C2C data, this fire has an estimated area of approximately 183,207 ha in 1989, with an additional 81,445 ha mapped in 1990. As indicated in Fig. 8, this fire burned for an extended period of time, beyond the image compositing end date of August 31 in 1989 (Fig. 8A), with additional burned areas visible in the 1990 composite (Fig. 8B). Moreover, the numerous unburned areas are visible, and neither these, nor the water bodies (black), are excluded from the CNFDB fire perimeter estimate. In the CNFDB database, this fire represents

Table 3
Relative ecozone contributions to national disturbance areas (1985–2010).

Ecozone	Contribution to total area disturbed by wildfire (%)	Contribution to total area disturbed by harvest (%)	Contribution to total area disturbed (%)
Atlantic Maritime	0.066	15.876	4.702
Boreal Cordillera	6.287	0.455	4.577
Boreal Plains	8.340	11.660	9.314
Boreal Shield East	8.667	37.620	17.157
Boreal Shield West	26.850	10.585	22.080
Hudson Plains	4.585	0.188	3.296
Montane Cordillera	1.476	17.311	6.119
Pacific Maritime	0.056	5.060	1.524
Taiga Cordillera	2.446	0.089	1.755
Taiga Plains	15.112	1.091	11.001
Taiga Shield East	9.324	0.040	6.602
Taiga Shield West	16.791	0.025	11.874

about 5% of the total area burned in 1989. The total area difference in the mapping of this single fire between the CNFDB and the C2C product was approximately 146,000 ha.

Differences between spatial estimates of area burned between the CNFDB and C2C appear to be greater in years when there is a larger total area disturbed by wildfire (Fig. 7). Indeed, the amount of wildfire area in a given year (as estimated by the CNFDB) explained a significant proportion of the variance in the absolute difference between C2C and CNFDB estimates of wildfire area ($R^2 = 0.692$, $F(1,24) = 53.94$, $p < 0.001$; Electronic Supplement Fig. S1). The years with the greatest difference between the CNFDB and the C2C fires were 1989, 1994, and 1998. As documented by Stocks et al. (2002), a relatively small number of fires in any given year often represent a large proportion of the total area disturbed by wildfire. In 1989, 1994, and 1998, approximately 3% of the fires in each year represented more than half of the total wildfire area (according to the CNFDB data). We summed the total amount of area identified as wildfire by C2C within the perimeters of the largest *N* fires for each of these years (that is, the *N* fires that accounted for at least 50% of the area disturbed by wildfire in that year). We found that on average, C2C identified 61% of these areas as being disturbed by wildfire (Table 4).

3.3. Characterizing vegetation recovery following wildfire and harvest

Nationally, in the first 5 years following disturbance, 13.2% of the areas disturbed by wildfire had an $\Delta NBR_{regrowth}$ value that was ≤0, compared to 14.4% of the areas disturbed by harvest (Fig. 9A), with the remaining areas disturbed by wildfire or harvest having positive $\Delta NBR_{regrowth}$ values, considered indicative of spectral recovery. The average national $\Delta NBR_{regrowth}$ value for wildfire was 0.36 ($\sigma = 0.22$) compared to 0.26 for harvest ($\sigma = 0.14$). The Taiga Cordillera ecozone had the largest mean $\Delta NBR_{regrowth}$ value following wildfire (0.45, $\sigma = 0.21$), while the Taiga Plains had the largest mean $\Delta NBR_{regrowth}$ value following harvest (0.33, $\sigma = 0.14$; Fig. 9B). Consistent with the national trend (Fig. 9A), mean $\Delta NBR_{regrowth}$ values for each ecozone were generally larger for wildfire compared to harvest, with the exception of the Pacific Maritime ecozone (Fig. 9B). In summary, the majority of areas (> 85%) disturbed by wildfire or harvest had positive $\Delta NBR_{regrowth}$

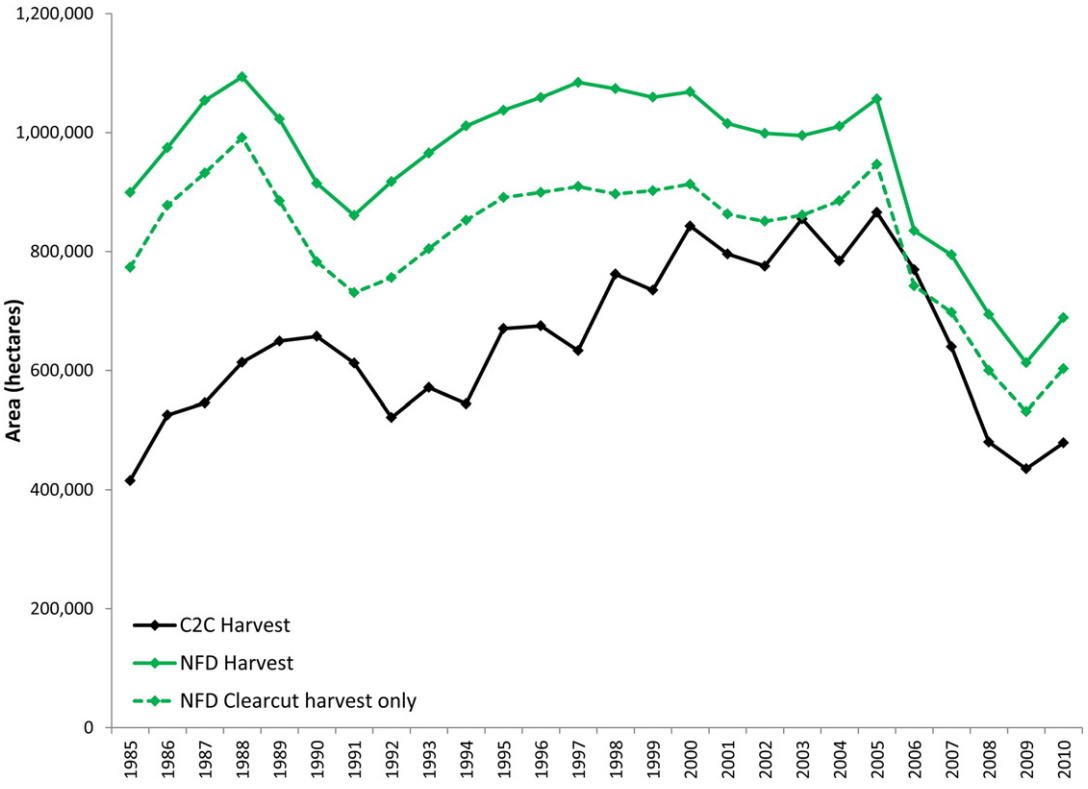

Fig. 6. Area harvested in Canada's forested ecosystems (1985–2010) as estimated by the aspatial National Forestry Database (NFD) and the Composite to Change (C2C) outputs.

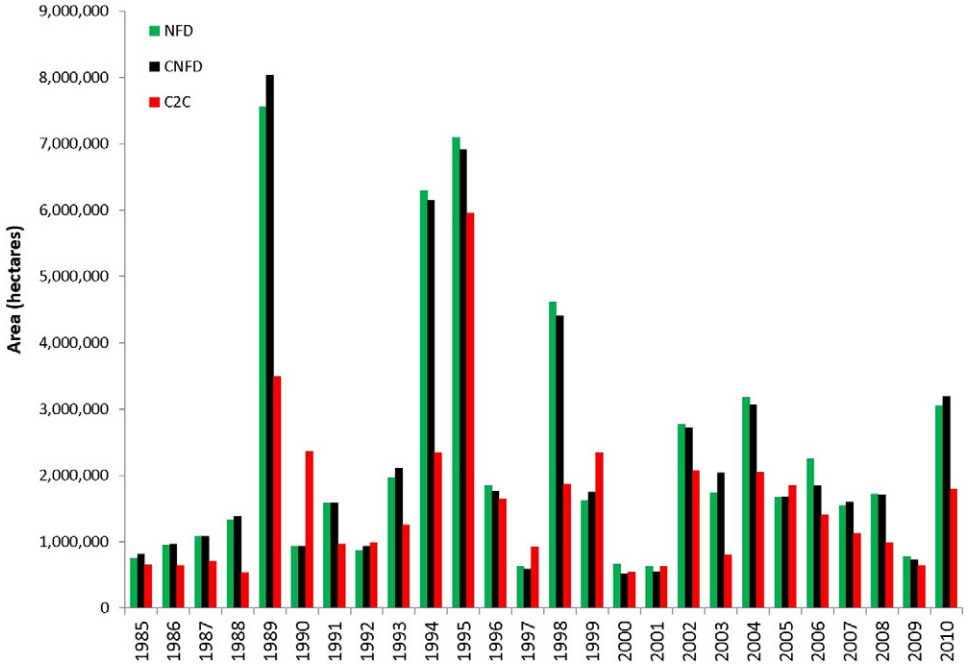

Fig. 7. Area of wildfire in Canada's forested ecosystems (1985–2010) as estimated by the National Forestry Database (NFD; aspatial), the Canadian National Fire Database (CNFDB; spatial), and the Composite to Change (C2C) outputs.

values. On average, wildfire areas had larger $\Delta NBR_{regrowth}$ values than areas disturbed by harvest, but the variability in $\Delta NBR_{regrowth}$ values for wildfire was also greater.

When $\Delta NBR_{regrowth}$ is scaled by the magnitude of the disturbance, a relative indicator of short-term recovery is generated (Recovery Indicator or RI). The average change magnitude or $\Delta NBR_{disturbance}$ for wildfire areas was 0.605 ($\sigma = 0.255$), compared to 0.425 ($\sigma = 0.172$) for harvest areas (Electronic Supplement Fig. S2). Once the magnitude of the disturbance is incorporated into the recovery metric, the amount of area that would be considered as non-recovering (i.e., ≤ 0) decreases relative to that indicated by $\Delta NBR_{regrowth}$ values: 4.3% of the wildfire areas and 6.1% of the harvest areas had an RI value ≤0 (Fig. 10A). Also, in contrast to trends observed for $\Delta NBR_{regrowth}$ values, wildfire areas generally had lower average RI values (0.55, $\sigma = 0.62$); compared to harvest areas (0.61, $\sigma = 0.67$; Fig. 9A). Nationally, 62.8% of the area disturbed by wildfire and 64.9% of area disturbed by harvest had an RI value ≥0.5. By ecozone, mean RI values are greater for harvesting for 7 of the 12 ecozones, and the standard deviations for mean ecozone RI values are larger than $\Delta NBR_{regrowth}$ for both wildfire and harvest (Fig. 10B). In summary, once the magnitude of the disturbance is considered, harvest areas had higher RI values on average than wildfire areas, ecozone differences between wildfire and harvest mean values were markedly lower, and the standard deviation increased for some ecozones (e.g., Boreal Cordillera) and decreased for others (e.g., Montane Cordillera).

Vegetation recovery following disturbance is a process that varies greatly in both time and space. A 5-year window, as measured by the $\Delta NBR_{regrowth}$ and RI metrics provides an initial assessment of conditions post disturbance. To evaluate recovery over a longer temporal window, we calculated how many years it took for a pixel to reach 80% of its pre-disturbance NBR value (Y2R). Approximately, 68.4% of wildfire areas and 92.5% of harvest areas attained an NBR value that was 80% of the pre-disturbance NBR value, by the end of the time series in 2010 (Fig. 11A). Note that this would include all disturbances that occurred between 1985 and 2005, so for some disturbances, there is only a 5-year period post-disturbance available for analysis. If we specifically consider those disturbances in our time

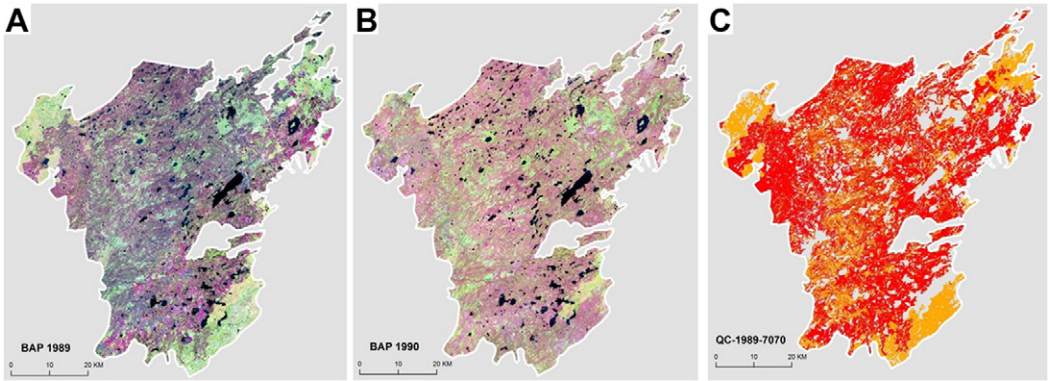

Fig. 8. The perimeter of fire QC-1989-7070 in northwestern Quebec, with the BAP proxy composite for 1989 (A) and 1990 (B). According to the CNFDB, this fire had an area of approximately 412,562 ha in 1989, and was the second largest wildfire in that year. This fire accounts for approximately 9% of the difference in total area between the CNFDB and C2C estimates of wildfire area in 1989. The same fire as mapped by the C2C approach shows that 183,207 ha were mapped as wildfire in 1989 (C; red), with an additional 81,445 ha of wildfire mapped in 1990 (C; orange). The CNFDB indicates that this fire was started by a lightning strike on June 24th, 1989.

Table 4
Spatial analysis of the largest fires in 1989, 1994, and 1998 (representing ~50% of area disturbed by wildfire in each of those years).

Comparative statistics	1989	1994	1998	Mean
Total wildfire area (CNFDB)	8,042,770	6,147,445	4,407,642	6,199,286
Total number of fires (CNFDB)	905	541	1084	843
Number of fires representing ~50% of total wildfire area (CNFDB)	24	17	28	23
Proportion of total fires analyzed (CNFDB)	2.65	3.14	2.58	2.79
Total wildfire area in largest fires (CNFDB)	4,145,039	3,147,943	2,243,078	3,178,687
Proportion of total wildfire area in largest fires (CNFDB)	51.54	51.21	50.89	51.28
Total wildfire area as estimated by (C2C)	3,492,391	2,345,749	1,866,035	2,568,058
Difference between CNFDB and C2C total area estimates of wildfire	4,550,379	3,801,696	2,541,607	3,631,227
Proportion of CNFDB wildfire area analyzed that was identified as C2C fire	53.19	63.92	66.08	61.06

series that have had the longest time period of recovery (i.e. if we consider only those disturbances that occurred prior to 1990), 86.3% of wildfire areas, and 98.4% of harvest areas attained an NBR value that was 80% of their respective pre-disturbance NBR (Fig. 11). This compares to 72.6% of wildfire areas and 96.1% of harvested areas for disturbances that occurred between 1990 and 2000. The national Y2R average value for wildfire areas was 10.6 years (σ = 5.6 years) compared to 6.6 years (σ = 3.9 years) for harvest areas.

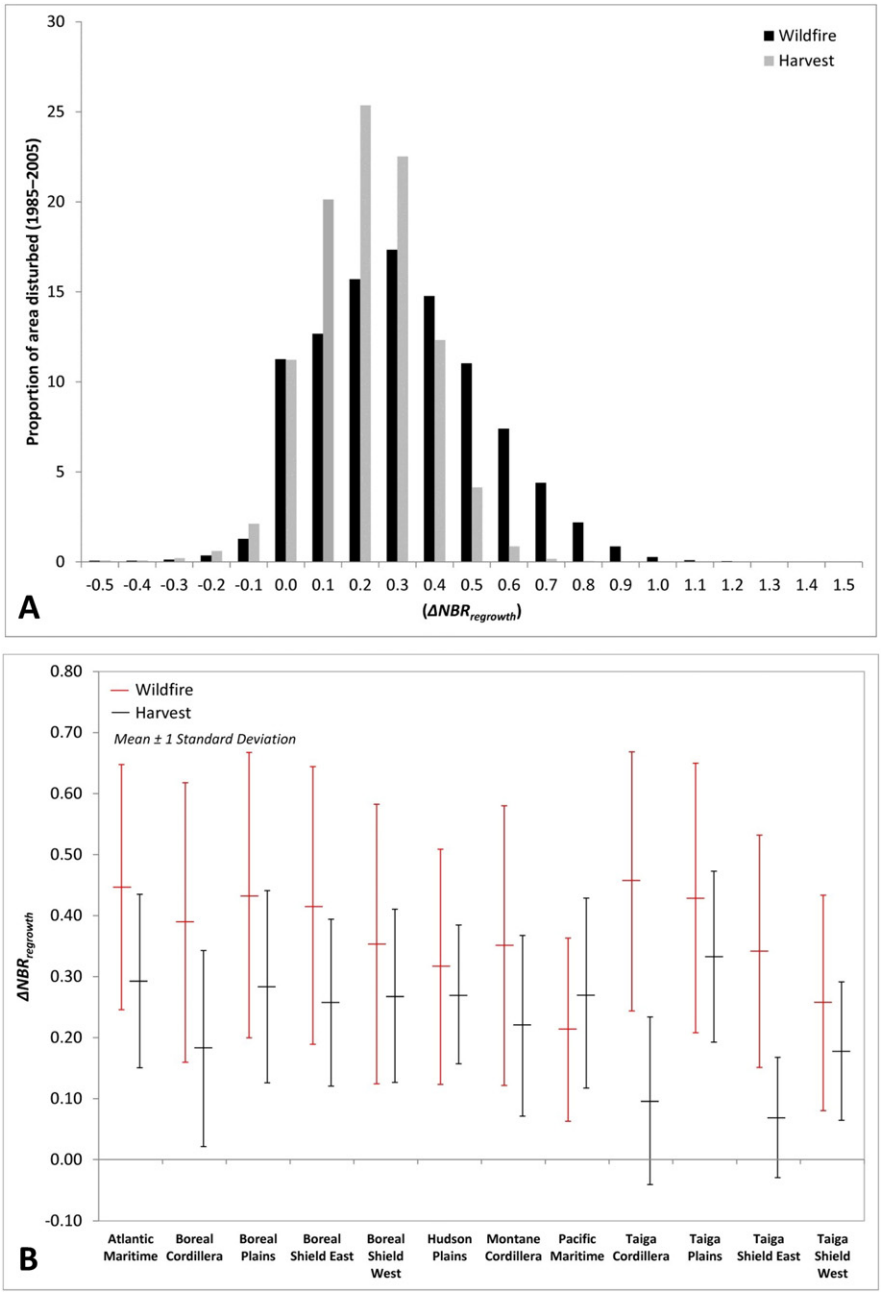

Fig. 9. National distribution of $\Delta NBR_{regrowth}$ values for wildfire and harvest (A) and ecozone mean $\Delta NBR_{regrowth} \pm 1$ standard deviation (B).

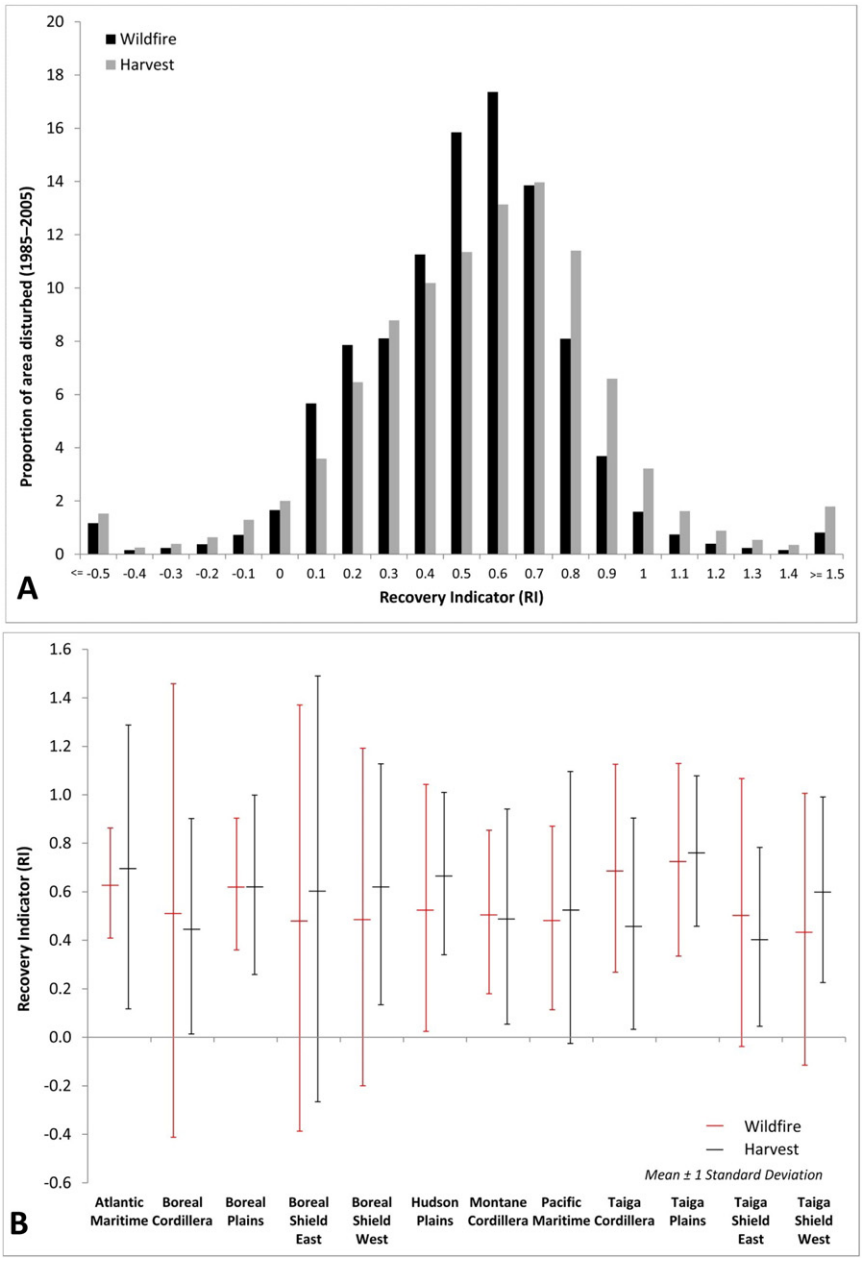

Fig. 10. National distribution of Recovery Indicator (RI) values for wildfire and harvest (A) and ecozone mean ± 1 standard deviation (B).

Overall, 35.5% of wildfire areas and 78.5% of harvest areas had a Y2R value ≤10 years. By ecozone, the Taiga Shield East had the longest average Y2R for wildfire (12.2 years, $\sigma = 6.1$ years), while the Montane Cordillera had the longest average Y2R for harvest (8.3 years, $\sigma = 4.8$ years) (Fig. 11B). In summary, harvested areas had lower average Y2R values than areas disturbed by wildfire. Differences in the rate at which pixels recovered from wildfire and harvest are shown in Fig. 12A and B, respectively.

The proportion of disturbed pixels that are considered non-recovering using the Y2R metric are provided by ecozone in Fig. 13. As per national trends, when all disturbance events are included (1985–2005), the proportion of disturbed areas that are considered as non-recovering at the end of the time series was greater than when only those disturbances occurring pre-1990 are considered. Therefore, Fig. 13 must be interpreted in the context of the temporal distribution of wildfire and harvest within each ecozone, as generalized by five-year epoch in Fig. 14. For example, the Montane Cordillera ecozone had the largest proportion (54.9%) of area disturbed by wildfire that was considered non-recovered with the Y2R metric; however, as indicated in Fig. 14, approximately one-third of the wildfire disturbance in this ecozone occurred later in the time series (2000–2004 epoch). Similarly, the Taiga Cordillera had the largest proportion of area disturbed by harvesting that was non-recovered by the end of the analysis period (Fig. 13); and almost half (by area) of the harvesting in this ecozone occurred between 1985 and 1989 (Fig. 14), suggesting that recovery following harvesting in this ecozone may be slower than other ecozones as a function of low productivity and a very short growing season in this northern ecozone (Table 1). Harvesting in the Taiga Cordillera is very minimal and certainly not commercially viable, representing only 0.003% of the net ecozone area disturbed annually (Electronic Supplement Table S1), and contributing just 0.089% to the total national area disturbed by harvest (Table 3). In contrast, the Boreal Shield East contributes 38% of the total national area disturbed by harvesting, and in this ecozone, characterized by high productivity and favourable growing conditions (Table 1) where forest harvesting is an important commercial activity, only 4.48% of areas disturbed by harvest (1985–

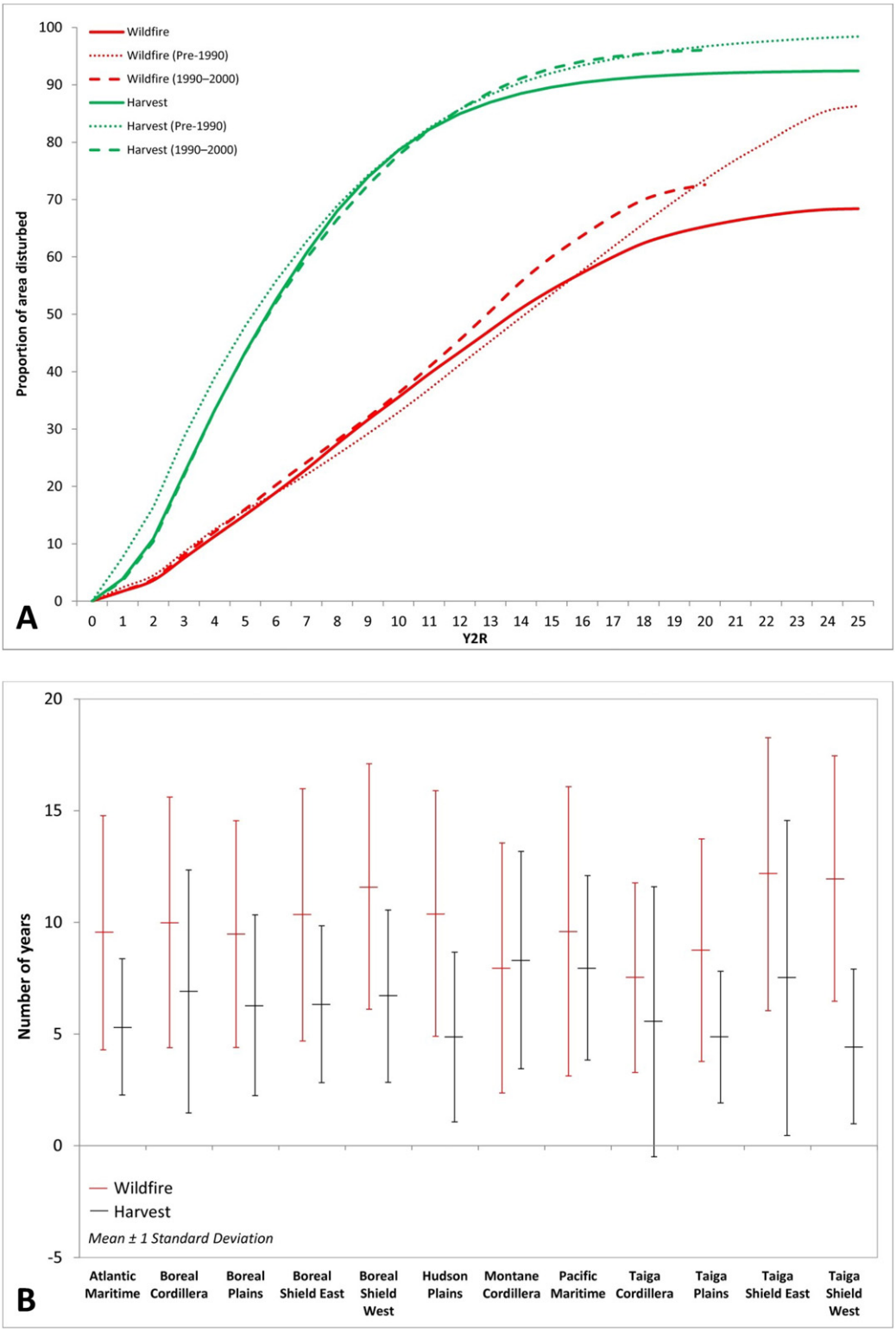

Fig. 11. National summary of Years to Recovery (Y2R) values for wildfire and harvest. (A) The cumulative proportion of area disturbed by Y2R is plotted for all disturbances (1985–2005), for disturbances that occured prior to 1990, and for disturbances that occurred between 1990 and 2000. Ecozone mean Y2R ± 1 standard deviation for all disturbances (1985–2005) are shown in (B).

2005), and only 0.11% of areas disturbed by harvest prior to 1990, were considered non-recovered using the Y2R metric (Fig. 13).

Overall, <1% of the areas disturbed by wildfire and harvest were identified as non-recovering by all three spectral measures of recovery used in our analysis (Table 5). Conversely, 77.4% of harvest areas and 57.4% of areas disturbed by wildfire were considered as recovered by all three metrics. Approximately 15% of areas that were disturbed by wildfire and harvest and identified as non-recovering by the short-term metrics, were recovered by the end of the time series. Of note, 28.7% of the areas disturbed by wildfire that were identified as recovering by the short-term metrics, had not yet recovered by the end of the time series in 2010; we found that approximately half of this area is located in areas

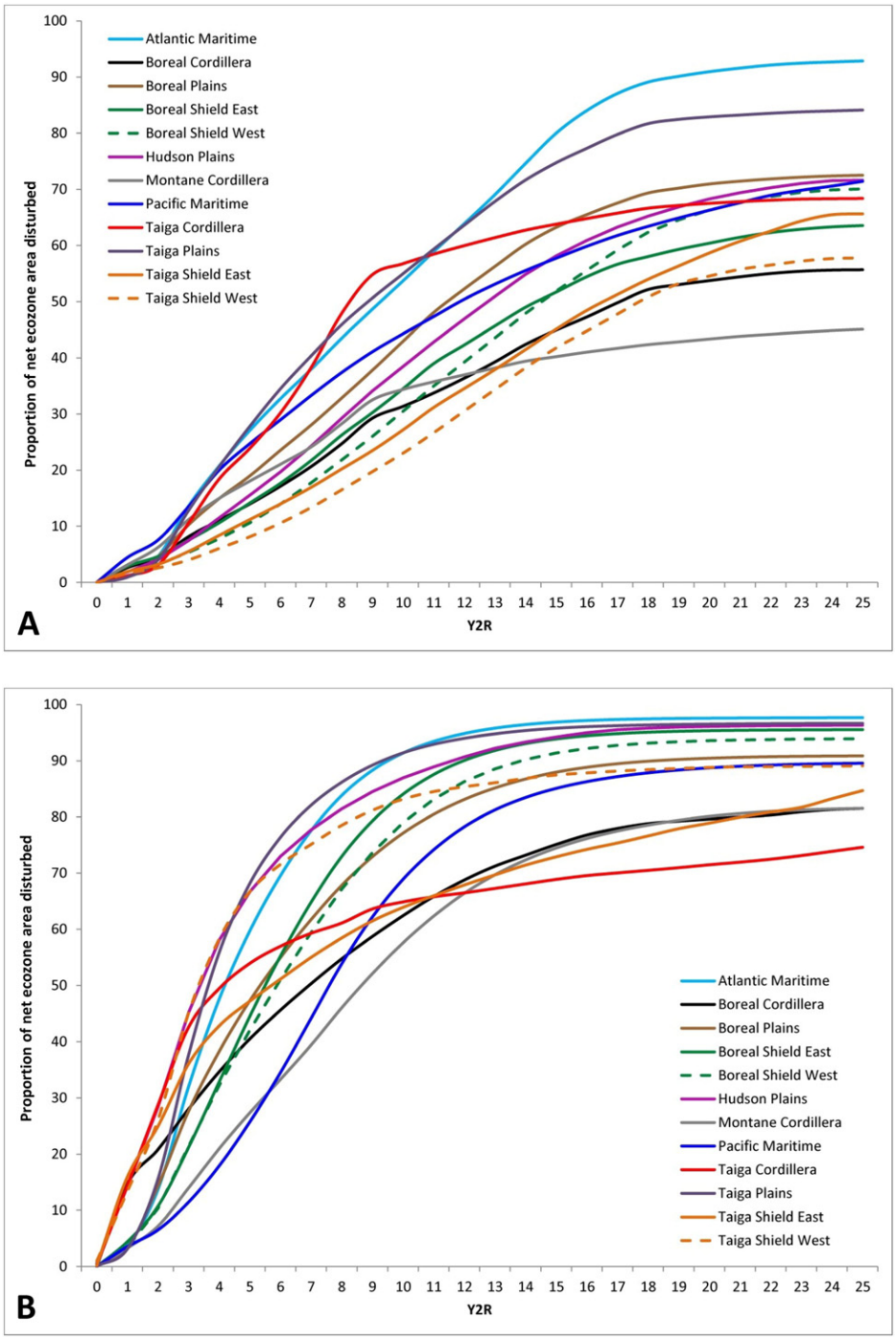

Fig. 12. Cumulative proportion of net ecozone area disturbed that has recovered, as measured using a longer-term indicator of spectral recovery, the Years to Recovery or Y2R, for wildfire (A) and harvest (B).

that were disturbed by wildfire prior to 2000, and 6.8% prior to 1990. By comparison, only 6.7% of areas disturbed by harvest that were identified as recovering by the short-term metrics, had not yet recovered by the end of the time series in 2010, and approximately 21% of this area was harvested prior to 2000, and only 3.2% prior to 1990.

4. Discussion

4.1. Disturbance by wildfire and harvest in Canada

The C2C data used in our analysis (Hermosilla et al., 2016) represent a nationally consistent and detailed depiction of wildfire and harvest for the period 1985–2010, at a spatial resolution that is relevant for forest management and monitoring. Herein, we used the C2C outputs to provide a national characterization of trends in disturbance and recovery, distinguished by disturbance type. We found that the total area disturbed by wildfire was almost 2.5 times that of the total area disturbed by harvesting and that wildfire has markedly greater inter-annual variability in terms of area disturbed. Indeed we found that almost one quarter of the total area disturbed by wildfire (23%) from 1985 to 2010 occurred in just two years (1989 and 1995). This year-to-year fluctuation in areas disturbed by fire was also noted by Stocks et al. (2002), who documented that the annual area burned in Canada fluctuated by more than an order of magnitude over the period 1970–1997,

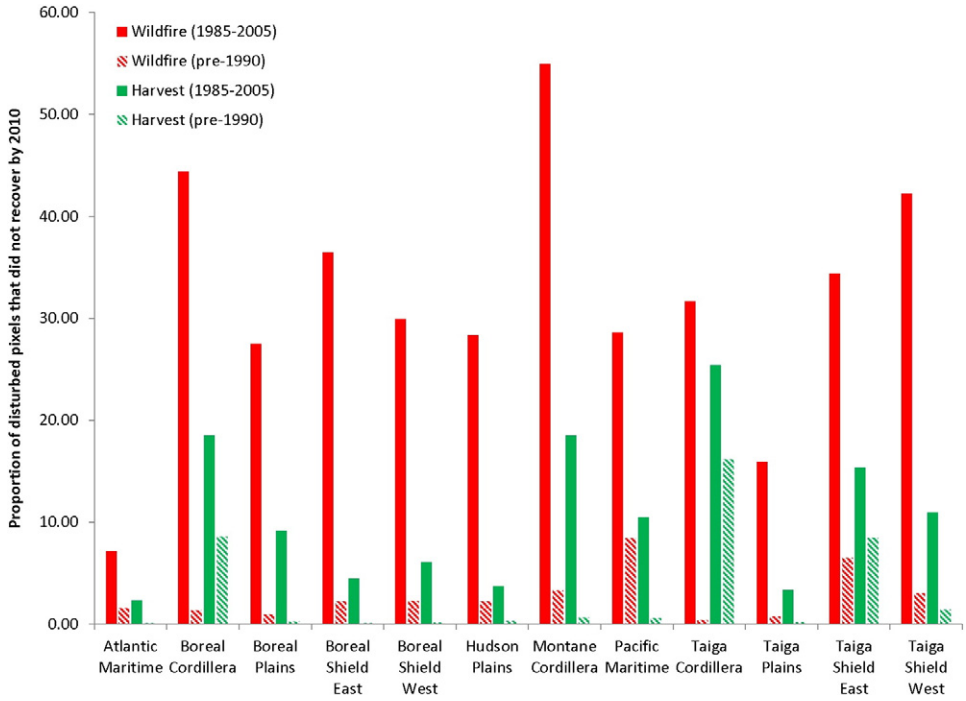

Fig. 13. Proportion of disturbed pixels, by ecozone, that are considered not recovered using the Years to Recovery (Y2R) metric (i.e. the pixel did not return to 80% of its pre-disturbance value by 2010).

representing a significant challenge to fire management agencies (Magnussen and Taylor, 2012). Through ecozone analysis, important regional differences emerged in the spatial distribution of wildfire and harvest across Canada's forested ecozones. Of particular note, the boreal ecozones had the greatest absolute area of disturbance from both wildfire (Boreal Shield West) and harvest (Boreal Shield East) (Table 2) and these two ecozones represented the greatest relative contribution (39%) to total area disturbed in Canada (1985–2010) (Table 3). Temporally, the greatest fire years, in terms of total area disturbed, occurred more than twenty years ago (1989 and 1995; Fig. 7). Ecozone trends in wildfire and harvest disturbance reflect a complex assemblage of factors including forest productivity, forest management, and population characteristics, among others (Table 1).

While the focus of this analysis was on stand replacing disturbance, it must be noted that other forms of disturbance (e.g. insects, water stress) can also play an important role in the dynamics of forested

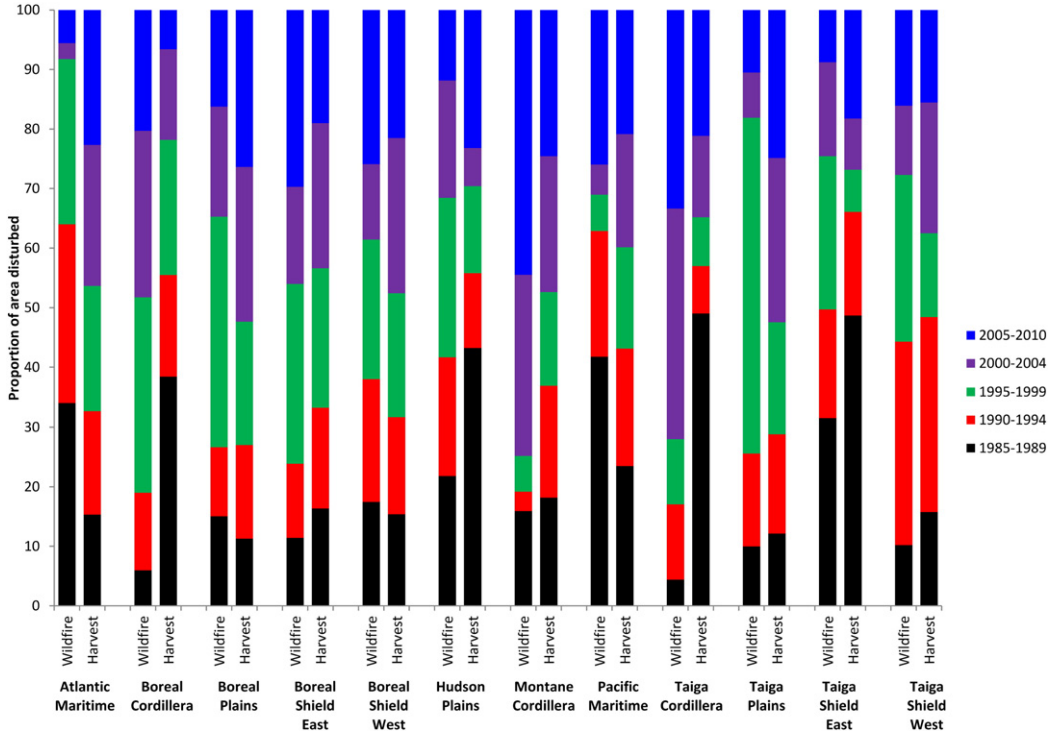

Fig. 14. Epochal (5-year) distribution of wildfire and harvest, by ecozone.

Table 5
Summary of a spatial overlay of the three spectral recovery metrics: ΔNBRregrowth, RI, and Y2R. A red circle indicates that the metric evaluated the pixel as "not recovered", while a green circle indicates that the metric evaluated the pixel as "recovered".

$\Delta NBR_{regrowth}$	RI	Y2R	Interpretation	Proportion of total area disturbed by wildfire 1985–2010	Proportion of total area disturbed by harvest 1985–2010
🟢	🟢	🟢	Recovery indicated by all 3 metrics	57.446	77.362
🟢	🟢	🔴	Short-term recovery indicated, long-term recovery not attained by 2010	28.766	6.708
🟢	🔴	🟢	Recovery indicated by $\Delta NBR_{regrowth}$ and Y2R	0.711	1.020
🟢	🔴	🔴	Recovery indicated by $\Delta NBR_{regrowth}$ only	0.124	0.071
🔴	🟢	🟢	Recovery indicated by RI and Y2R	0.134	0.173
🔴	🟢	🔴	Recovery indicated by RI only	0.003	0.002
🔴	🔴	🟢	Long-term recovery indicated	11.891	13.671
🔴	🔴	🔴	No recovery was indicated by any of the metrics	0.927	0.992

ecosystems and can have significant impacts on applications such as carbon accounting (Kurz et al., 2008). While some insect disturbances manifest in ways that are relatively abrupt and readily detectable (e.g. bark beetles) others are more ephemeral (e.g. defoliators) and although separating the two has been demonstrated (Senf et al., 2015), it is challenging to do so in a national context, where there are many potential and region-specific (and often overlapping) insects and pathogens present. The capacity to use Landsat time series analysis to characterize these various non-stand replacing disturbances is emerging (e.g. Cohen et al., 2016, Vogelmann et al., 2016); however, spectral measures of recovery from these non-stand replacing changes have yet to be explored and will require further consideration and research.

4.2. Comparison to existing national disturbance data for Canada

A comparison of C2C outcomes to existing data products must take into consideration the differences in how estimates are currently derived, including mapping methods and the spatial resolution of the data used, among others. In the case of harvests, much of the earlier data used to report national trends in harvesting over time was aspatial. Methods for recording harvest information have evolved over time as GIS technology has become ubiquitous in natural resource management agencies (Leckie and Gillis, 1995). In the case of wildfire, the mapped outcomes are expected to differ, based on known differences in the methods applied and data used, especially as related to differences in source data spatial resolution, definitions of minimum mapable units, and treatment of unburned islands and waterbodies within wildfire boundaries (e.g., Fraser et al., 2004).

While some jurisdictions in Canada do maintain a spatial record of harvesting activity, the quality and spatial and temporal extent of these data are not consistent (Gillis and Leckie, 1996). As such, the Landsat time series data offers a unique opportunity to provide a synoptic, nationally consistent perspective of stand-replacing harvest over a longer time window. While not relevant for all jurisdictions, additional research is required to determine the nature and capacity for detection of non-clearcut forms of harvesting using Landsat time series (e.g., Healey et al., 2006; Jarron et al., 2017). In a study that compiled data on harvesting across North America, Masek et al. (2011) identified jurisdictions in Canada with the largest amount of harvest, by area: Québec, Ontario, and British Columbia. We found similar trends, with 48.2% of the total national area disturbed by harvesting found in the Boreal Shield East and West (Quebec and Ontario) and 22.7% in the Montane Cordillera, Pacific Maritime, and Boreal Cordillera ecozones (British Columbia). Nationally, the annual area harvested in Canada estimated using NFD has remained relatively stable over the period considered, whereas the C2C data indicates an increase in harvesting, from approximately 415,000 ha in 1985 to 866,000 ha in 2005 (Fig. 6). Harvest levels are expected to vary over time, with fluctuations resulting from changes in market demand for wood products or from salvage harvesting associated with large disturbance events such as the mountain pine beetle outbreak in western Canada in the 2000s (Kurz et al., 2008). While the C2C data were subject to two independent accuracy assessments (Hermosilla et al., 2015b, 2016), the NFD data has not been assessed, nor is such an assessment possible in the absence of any independent spatial reference dataset. As a result, a full explanation of the difference in the long-term trends in harvest levels shown in Fig. 6 is not possible. Masek et al. (2011) did identify an increasing trend in harvest levels in certain jurisdictions, such as Quebec, and this is reflected in the NFD data for that jurisdiction. In part, this difference in trends may be partially attributable to the particular qualities of the NFD data, as previously identified in Section 2.2.2. Of note, as mapping methods have advanced over time and GIS data have become more commonly used by forest management agencies (Gillis and Leckie, 1996), there is increasing correspondence between the C2C estimates and those of the NFD.

Comparison of the C2C-derived trends for disturbance by wildfire and harvest to existing data used for national reporting allows for improved understanding of the relative differences between the various information products. Of note, the largest differences between the CNFDB and C2C occur in the years with the greatest amount of wildfire. These large fires would be particularly difficult to map accurately via a method such as hand sketching, especially in years where there are many large fires across the landscape. An example of this is provided in Fig. 8, which illustrates the differences in fire areas captured by the CNFDB and C2C for a single fire in 1989. Another factor that may contribute to the differences observed between the C2C and CNFDB product is associated with the rules used to generate the Landsat image composites (White et al., 2014). The target day of year used for compositing is August 1 $\pm$ 30 days. As such fires that occur in September or later would not be detected by the C2C process until the following year. This latency in detection can be observed in Fig. 8A and B for 1989 and 1990. A query against the CNFDB database indicates that <1% of fires, by area, in 1989 and 1994 have a report date after August 31. Also worth noting is that this query is based on report date, and fires can burn for weeks or months thereafter, in which case areas disturbed post-August 31 would not be identified in the C2C product until the following year.

4.3. Characterizing vegetation recovery

The C2C data provides an unprecedented opportunity to characterize variability in post-disturbance vegetation recovery in Canada's forested ecosystems in a consistent and systematic fashion by ecozone and disturbance type. The potential capacity of Landsat time series data to monitor post-disturbance recovery was established some twenty years ago (e.g. Viedma et al., 1997); however implementation was constrained by issues related to both data and computation. Today, the use of Landsat time series to assess post-disturbance recovery has been greatly facilitated by free and open access to the Landsat archive (Woodcock et al., 2008) and advances in computational capabilities. Research on spectral measures of forest recovery have emphasized the use of multiple metrics to provide a comprehensive assessment of recovery (Pickell et al., 2016; Chu et al., 2016). Challenges have been associated with using metrics such as NDVI that can saturate in as little as two years post-disturbance with the initial flush of herbaceous vegetation that often follows disturbance in some forest environments (Buma, 2012). Also critical to understanding vegetation recovery post-disturbance is the variability in recovery trends across forested ecosystems, which for a country like Canada with such a large and diverse range of forest conditions, is difficult to quantify on the basis of a small number of field plots alone (Bartels et al., 2016).

Depending on their severity and form, wildfires can leave substantial residual vegetation at a site (Johnstone and Kasischke, 2005), or when intense, can kill all live biomass (Seedre et al., 2014). Residual vegetation can also remain after harvesting, in the form of wildlife trees, seed trees, or advanced regeneration (Seedre et al., 2014). Given the greater variability in magnitude associated with fire that we observed (and associated variability in residual vegetation post-disturbance), it is perhaps not surprising that over the short-term, we found that wildfire areas had more rapid spectral recovery post-disturbance than areas disturbed by harvesting. Indeed, ground-based studies would indicate that the majority of tree establishment occurs within 3 to 10 years post fire (Lavoie and Sirois, 1998; Gutsell and Johnson, 2002; Johnstone et al., 2004; Bartels et al., 2016). Our longer-term measure of spectral recovery (Y2R) indicated that harvested areas are recovering more strongly over the longer term, with 78.6% of areas disturbed by harvest having a Y2R value ≤10 years, compared to only 35.5% of areas disturbed by wildfire. Nationally, 92.5% of harvest areas and 68.4%% of wildfire areas had reached our designated Y2R benchmark of recovery by the end of the time series (Fig. 11). By definition, harvesting impacts a more limited set of land cover types, occurs on more productive sites, and is more likely, through management intervention, to return rapidly to a forested state. What also must be considered is the potential for the composition of the forests to change post-disturbance, such as the post-wildfire shift from *Picea* to *Pinus* communities reported by Lavoie and Sirois (1998), that may also impact any measure of longer-term spectral recovery.

Past research characterizing national trends in post-disturbance recovery in Canada have primarily used AVHRR data (Amiro et al., 2000; Hicke et al., 2003; Goetz et al., 2006). Nationally, our long-term recovery metric, Y2R, had a mean of 12.2 years for areas disturbed by wildfire. This compares to a national mean post-fire recovery time of 9 years reported by Hicke et al. (2003) and 5 years reported by Goetz et al. (2006). Amiro et al. (2000) found a lower increase in NPP for the Taiga Shield relative to the Boreal Shield. We found similar trends between these two ecozones for recovery post-fire, but noted differences in post-harvest recovery for the Taiga Shield East, for both short (Fig. 9) and long-term (Fig. 12) recovery metrics. The Taiga Shield East has a shorter growing season relative to the Taiga Shield West and Boreal Shield East and West (Table 1). In the context of this past work, the results presented herein offer insights on the relative rates of recovery across Canada's diverse forested ecozones for both wildfire and harvest, providing a detailed characterization of both regional and national trends.

Frazier et al. (2015) used Landsat Tasseled Cap components for a sample-based assessment (8 Landsat scenes) of recovery in the Western and Eastern Boreal Shield using Landsat time series (1984–2013). The authors postulated that the stronger recovery response they found in the Eastern Boreal ecozone may be attributable to differences in pioneer vegetation, climatic variables, soil conditions, and disturbance frequency and size. The results of our wall-to-wall analysis of approximately the same time period, indicate that the Western Boreal Shield had 2.8 Mha more disturbance than the Eastern Boreal Shield, and that the Western Boreal Shield was dominated by wildfire (86.1%), while the Eastern Boreal Shield was dominated by harvest (63.8%). At the end of the time series, the proportion of pixels that had recovered was very similar for harvested areas (83.8% and 84.6% for East and West respectively), and less similar for areas disturbed by wildfire (55.6% and 65.6% for East and West respectively). While differences in pioneer vegetation types likely would have an impact on spectral recovery trajectories, as suggested by Frazier et al. (2015), we hypothesize that the differences in recovery rates observed by Frazier et al. (2015) were driven primarily by disturbance type. Frazier et al. (2015) did not account for disturbance type in their comparative assessment of recovery and their samples in the Boreal Shield East were predominantly located in the managed forest, where harvesting is much more prevalent, whereas their samples in the Boreal Shield West were predominantly located in the unmanaged forest, where harvesting is much less likely to occur. As noted above, harvesting typically occurs on more productive sites whereas fires can occur anywhere and as a result often encompass more heterogeneous environments. Our hypothesis of the importance of disturbance type to understanding recovery trends is corroborated by a recent study in the Boreal Shield East by Madoui et al. (2015), who found that productivity was a main driver in explaining the differences in recovery rates between areas disturbed by harvest and wildfire. Therein, the authors found that revegetation was more rapid for areas disturbed by harvest than fire; however, results were comparable for productive forest areas within burned areas and harvested areas.

Many of the aforementioned studies using Landsat time series data in a Canadian forest context were either sample-based (e.g., Frazier et al., 2015; Pickell et al., 2016) or have included only a single or a small number of disturbance events (e.g., Chu et al., 2016; Ireland and Petropoulos, 2015) or were limited to a specific region (e.g., Madoui et al., 2015). There have been few studies that have used Landsat time series data to characterize both disturbance and recovery trends, in a spatially-explicit manner, over very large forest areas. Kennedy et al. (2012) characterized both disturbance and recovery for a 23 Mha area of the US Pacific Northwest from 1985 to 2008. The authors used both absolute and relative metrics of recovery, based on the NBR to characterize the spatial and temporal patterns of post-disturbance vegetation regrowth. Griffiths et al. (2014) likewise characterized forest disturbance and recovery for the 39 Mha Carpathian ecoregion from 1985 to 2010 using Landsat best-available-pixel (BAP) composites. In that study, authors used the Disturbance Index (DI; Healey et al., 2005) to develop an indicator of spectral recovery. Of note, neither Kennedy et al. (2012) nor Griffiths et al. (2014) distinguished trends in recovery by disturbance type. Thus, unique to the work presented herein was to use the historic Landsat record to provide a wall-to-wall, national, synoptic assessment of wildfire and harvest for the past 25 years for the ~650 Mha representing Canada's forested ecosystems, and to characterize trends in post-disturbance recovery by both disturbance type and ecozone.

5. Conclusions

Baseline data on forest change are essential for forest monitoring and understanding possible impacts of climate change, but they are difficult to compile from historical sources, which are frequently aspatial, spatially limited and/or have limited spatial detail, inconsistent (across large areas), or of limited temporal reach. The nature and quality of

the data available for monitoring purposes has changed markedly over the past three decades. Landsat time series offers a new opportunity to retrospectively generate these baseline data in a consistent manner over very large areas. Landsat-established baselines and subsequent trends provide a framework to augment and integrate existing information, including ground measurements. Such baseline information is important for identifying spatial and temporal trends regarding forest disturbance and recovery that can be used to inform and bound questions related to forest management and climate change.

Our results indicate that disturbance typing is critical for understanding trends in post-disturbance recovery. While methods for mapping stand replacing disturbance with earth observation data, particularly Landsat, are mature, the automated attribution of disturbance to a type or causal agent is nascent by comparison. The study of vegetation recovery using Landsat time series data is becoming increasingly common. With the now multi-decadal length of the Landsat record and the rigorous sensor cross-calibration of the Landsat program (Markham and Helder, 2012), recovery characterizations can add value to forest monitoring programs and science. The capacity to freely access and manipulate these data over long time frames and large areas has created new opportunities for monitoring not only disturbance, but vegetation response to disturbance, enabling an improved characterization of the long-term impacts of forest change. Such information is key for understanding the sustainability of forest management practices, as well as for understanding the potential for biomass uptake and carbon sequestration in these young forests. Overall, we found that <1% of the areas disturbed by wildfire and harvest (1985–2005) were concurrently identified as non-recovering by all three spectral measures of recovery used in our analysis. As noted by Griffiths et al. (2014), analyses of forest recovery driven by remote sensing would benefit from additional research focusing on the linkages between trends in spectral metrics of recovery and related development of forest structure.

Going forward, Landsat 8 and Sentinel 2, independently and especially when considered as part of a virtual constellation (Wulder et al., 2015), offer new opportunities for forest monitoring and extension of the baseline data presented herein. Both the Landsat 8 and Sentinel 2 programs are considered as operational, meaning that a key element of each program is measurement continuity. This operational capacity and commitment to measurement continuity (Wulder et al., 2016) is particularly useful for planning and implementation of monitoring programs. While of obvious value for a large, multi-jurisdictional nation such as Canada, the capability for annual wall-to-wall monitoring of forest change at a spatial scale that is relevant for forest management provides for consistent and transparent information across management or political boundaries and allows for a more systematic understanding of disturbance dynamics over large areas. As such, the human-scale monitoring capacity demonstrated herein is transferable to other jurisdictions with similar Landsat data availability, and has global relevance in the context of changing climate and increasing pressures on forest ecosystems.

6. Acknowledgements

This research was undertaken as part of the 'National Terrestrial Ecosystem Monitoring System (NTEMS): Timely and detailed national cross-sector monitoring for Canada' project jointly funded by the Canadian Space Agency (CSA) Government Related Initiatives Program (GRIP, #13MOA41002), and the Canadian Forest Service (CFS) of Natural Resources Canada, with additional support from a Natural Sciences and Engineering Research Council (NSERC, RGPIN 311926-13) Discovery Grant to N. Coops. Doug Bolton is thanked for compiling and processing the ecozone summaries of the MODIS GPP data.

Appendix A. Supplementary data

Supplementary data to this article can be found online at http://dx.doi.org/10.1016/j.rse.2017.03.035.

References

Amiro, B.D., Chen, M., Liu, J., 2000. Net primary productivity following forest fire for Canadian ecoregions. Can. J. For. Res. 30, 939–947.
Anderson-Teixeira, K.J., Miller, A.D., Mohan, J.E., Hudiburg, T.W., Duval, B.D., DeLucia, E.H., 2013. Altered dynamics of forest recovery under a changing climate. Glob. Chang. Biol. 19, 2001–2021.
Banskota, A., Kayastha, N., Falkowski, M.J., Wulder, M.A., Froese, R.E., White, J.C., 2014. Forest monitoring using Landsat time-series data: A review. 2015. Can. J. Remote. Sens. 40 (5), 362–384.
Bartels, S.F., Chen, H.Y.H., Wulder, M.A., White, J.C., 2016. Trends in post-disturbance recovery rates of Canada's forests following wildfire and harvest. For. Ecol. Manag. 361:194–207. http://dx.doi.org/10.1016/j.foreco.2015.11.015.
Bolton, D.K., Coops, N.C., Wulder, M.A., 2015. Characterizing residual structure and forest recovery following high-severity fire in the western boreal of Canada using Landsat time-series and airborne LiDAR data. Remote Sens. Environ. 163, 48–60.
Breiman, L., 2001. Random forests. Mach. Learn. 45 (1), 5–32.
Buma, B., 2012. Evaluating the utility and seasonality of NDVI values for assessing post-disturbance recovery in a subalpine forest. Environ. Monit. Assess. 184, 3849–3860.
Canadian Forest Service, 2015. Canadian National Fire Database – Agency Fire Data. Natural Resources Canada, Canadian Forest Service, Northern Forestry Centre, Edmonton, Alberta. Available online http://cwfis.cfs.nrcan.gc.ca/ha/nfdb Accessed January 4, 2016.
Chu, T., Guo, X., 2014. Remote sensing techniques in monitoring post-fire effects and patterns of forest recovery in boreal forest regions: A review. Remote Sens. 6, 470–520.
Chu, T., Guo, X., Takeda, K., 2016. Remote sensing approach to detect post-fire vegetation regrowth in Siberian boreal larch forest. Ecol. Indic. 62, 32–46.
Cohen, W.B., Goward, S.N., 2004. Landsat's role in ecological applications of remote sensing. Bioscience 54, 535–545.
Cohen, W.B., Yang, Z., Kennedy, R., 2010. Detecting trends in forest disturbance and recovery using yearly Landsat time series: 2. TimeSync — Tools for calibration and validation. *Remote Sensing of Environment*. 114 pp. 2911–2924.
Cohen, W.B., Yang, Z., Stehman, S.V., Schroeder, T.A., Bell, D.M., Masek, J.G., Huang, C., Meigs, G.W., 2016. Forest disturbance across the conterminous United States from 1985–2012: the emerging dominance of forest decline. For. Ecol. Manag. 360, 242–252.
Dale, V.H., Joyce, L.A., McNulty, S., Neilson, R.P., Ayres, M.P., Flannigan, M.D., Hanson, P.J., Irland, L.C., Lugo, A.E., Peterson, C.J., Simberloff, D., Swanson, F.J., Stocks, B.J., Wotton, B.M., 2001. Climate change and forest disturbances. Bioscience 51, 723–734.
DeVries, B., Decuyper, M., Verbesselt, J., Zeileis, A., Herold, M., Joseph, S., 2015. Tracking disturbance-regrowth dynamics in tropical forests using structural change detection and Landsat time series. Remote Sens. Environ. 169, 320–334.
Ecological Stratification Working Group. 1996. A national ecological framework for Canada. Ottawa, ON: Agriculture and Agri-Food Canada and Environment Canada (Available from: http://sis.agr.gc.ca/cansis/publications/ecostrat/cad_report.pdf [cited on May 12th 2016]).
Epting, J., Verbyla, D., 2005. Landscape-level interactions of prefire vegetation, burn severity, and postfire vegetation over a 16-year period in interior Alaska. Can. J. For. Res. 35, 1367–1377.
Escuin, S., Navarro, R., Fernández, P., 2008. Fire severity assessment by using NBR (normalized Burn ratio) and NDVI (normalized difference vegetation index) derived from Landsat TM/ETM images. Int. J. Remote Sens. 29, 1053–1073.
Fraser, R.H., Hall, R.J., Landry, R., Lynham, T., Raymond, D., Lee, B., Li, Z., 2004. Validation and calibration of Canada-wide coarse resolution satellite burned-area maps. Photogramm. Eng. Remote. Sens. 70, 451–460.
Frazier, R.J., Coops, N.C., Wulder, M.A., 2015. Boreal shield forest disturbance and recovery trends using Landsat time series. Remote Sens. Environ. 170:317–327. http://dx.doi.org/10.1016/j.rse.2015.09.0150034-4257.
Frolking, S., Palace, M.W., Clark, D.B., Chambers, J.Q., Shugart, H.H., Hurtt, G.C., 2009. Forest disturbance and recovery: a general review in the context of spaceborne remote sensing of impacts on aboveground biomass and canopy structure. J. Geophys. Res. 114:1–27. http://dx.doi.org/10.1029/2008JG000911.
Gillis, M.D., Leckie, D.G., 1996. Forest inventory update in Canada. For. Chron. 72 (2), 138–156.
Gitas, I.Z., Mitri, G., Veraverbeke, S., Polychronaki, A., 2012. Advances in remote sensing of post-fire vegetation recovery monitoring—a review. Chapter 7. In: Fatoyinbo, L. (Ed.), Remote Sensing of Biomass - Principles and Applications. InTech http://dx.doi.org/10.5772/20571 Available from:. http://www.intechopen.com/books/remote-sensing-of-biomass-principles-and-applications/advances-in-remote-sensing-of-post-fire-monitoring-a-review.
Goetz, S., Fiske, G.J., Bunn, A.G., 2006. Using satellite time-series data sets to analyze fire disturbance and forest recovery across Canada. Remote Sens. Environ. 101, 352–365.
Gómez, C., White, J.C., Wulder, M.A., 2011. Characterizing the state and processes of change in a dynamic forest environment using hierarchical spatio-temporal segmentation. Remote Sens. Environ. 115, 1665–1679.
Griffiths, P., Kuemmerle, T., Baumann, M., Radeloff, V.C., Abrudan, I.V., Lieskovsky, J., Munteanu, C., Ostapowicz, K., Hostert, P., 2014. Forest disturbances, forest recovery, and changes in forest types across the Carpathian ecoregion from 1985 to 2010 based on Landsat image composites. Remote Sens. Environ. 151, 72–88.
Gutsell, S.L., Johnson, E.A., 2002. Accurately ageing trees and examining their height-growth rates: implications for interpreting forest dynamics. J. Ecol. 90, 153–166.
Hansen, M.C., Loveland, T.R., 2012. A review of large area monitoring of land cover change using Landsat data. Remote Sens. Environ. 122, 66–74.
Hansen, M.C., Potapov, P.V., Moore, R., Hancher, M., Turubanova, S.A., Tyukavina, A., Thau, D., Stehman, S.V., Goetz, S.J., Loveland, T.R., Kommareddy, A., Egorov, A., Chini, L., Justice, C.O., Townshend, J.R.G., 2013. High-resolution global maps of 21st-century forest cover change. Science 342, 850–853.

Healey, S.P., Cohen, W.B., Yang, Z.Q., Krankina, O.N., 2005. Comparison of tasseled cap-based Landsat data structures for use in forest disturbance detection. Remote Sens. Environ. 97:301–310. http://dx.doi.org/10.1016/j.rse.2005.05.009.

Healey, S.P., Yang, Z., Cohen, W.B., Pierce, D.J., 2006. Application of two regression-based methods to estimate the effects of partial harvest on forest structure using Landsat data. Remote Sens. Environ. 101, 115–126.

Hermosilla, T., Wulder, M.A., White, J.C., Coops, N.C., Hobart, G.W., 2015a. An integrated Landsat time series protocol for change detection and generation of annual gap-free surface reflectance composites. Remote Sens. Environ. 158, 220–234.

Hermosilla, T., Wulder, M.A., White, J.C., Coops, N.C., Hobart, G.W., 2015b. Regional detection, characterization, and attribution of annual forest change from 1984 to 2012 using Landsat-derived time-series metrics. Remote Sens. Environ. 170, 121–132.

Hermosilla, T., Wulder, M.A., White, J.C., Coops, N.C., Hobart, G.W., Campbell, L.B., 2016. Mass data processing of time series Landsat imagery: pixels to data products. Int. J. Digital Earth http://dx.doi.org/10.1080/17538947.2016.1187673.

Hicke, J.A., Asner, G.P., Kasischke, E.S., French, N.H.F., Randerson, J.T., Collatz, G.J., Stocks, B.J., Tucker, C.J., Los, S.O., Field, C.B., 2003. Postfire response of North American boreal forest net primary productivity analyzed with satellite observations. Glob. Chang. Biol. 9, 1145–1157.

Hicke, J.A., Allen, C.D., Desai, A.R., Dietze, M.C., Hall, R.J., Hogg, E.H.T., Kashian, D.M., Moore, D., Raffa, K.F., Sturrock, R.N., Vogelmann, J., 2012. Effects of biotic disturbances on forest carbon cycling in the United States and Canada. Glob. Chang. Biol. 18, 7–34.

Hofgaard, A., Tardif, J., Bergeron, Y., 1999. Dendroclimatic response of *Picea mariana* and *Pinus banksiana* along a latitudinal gradient in the eastern Canadian boreal forest. Can. J. For. Res. 29, 1333–1346.

Horler, D., Ahern, F., 1986. Forestry information content of Thematic Mapper data. Int. J. Remote Sens. 7, 405–428.

Ireland, G., Petropoulos, G.P., 2015. Exploring the relationships between post-fire vegetation regeneration dynamics, topography and burn severity: a case study from the Montane Cordillera Ecozones of Western Canada. Appl. Geogr. 56, 232–248.

Jarron, L.R., Hermosilla, T., Coops, N.C., Wulder, M.A., White, J.C., Hobart, G., Leckie, D.G., 2017. Differentiation of alternate harvesting practices using annual time series of Landsat data. Forests 8 (1). http://dx.doi.org/10.3390/f8010015.

Johnstone, J., Kasischke, E.S., 2005. Stand-level effects of soil burn severity on postfire regeneration in a recently burned black spruce forest. Can. J. For. Res. 35, 2151–2163.

Johnstone, J., Chapin, F.S., Foote, J., Kemmett, S., Price, K., Viereck, L., 2004. Decadal observations of tree regeneration following fire in boreal forests. Can. J. For. Res. 34, 267–273.

Kennedy, R.E., Yang, Z., Cohen, W.B., 2010. Detecting trends in forest disturbance and recovery using yearly Landsat time series: 1. LandTrendr — Temporal segmentation algorithms. Remote Sens. Environ. 114, 2897–2910.

Kennedy, R.E., Yang, Z., Cohen, W.B., Pfaff, E., Braaten, J., Nelson, P., 2012. Spatial and temporal patterns of Forest disturbance and regrowth within the area of the northwest forest plan. Remote Sens. Environ. 122, 117–133.

Keogh, E., Chu, S., Hart, D., Pazzani, M., 2001. An Online Algorithm for Segmenting Time Series. Proceedings IEEE International Conference on Data Mining, 2001. ICDM 2001, pp. 289–296.

Key, C.H., Benson, N.C., 2006. Landscape Assessment (LA). FIREMON: Fire effects monitoring and inventory system. In: Lutes, D.C., Keane, R.E., Carati, J.F., Key, C.H., Benson, N.C., Gangi, L.J. (Eds.), General technical report RMRS-GTR-164-CD (pp. LA — 1-55). USDA Forest Service, Rocky Mountains Research Station, Fort Collins, CO.

Kurz, W.A., Stinson, G., Rampley, G.J., Dymond, C.C., Neilson, E.T., 2008. Risk of natural disturbances makes future contribution of Canada's forests to the global carbon cycle highly uncertain. Proc. Natl. Acad. Sci. 105 (5), 1551–1555.

Lavoie, L., Sirois, L., 1998. Vegetation changes caused by recent fires in the northern boreal forest of eastern Canada. J. Veg. Sci. 9, 483–492.

Leckie, D.G., Gillis, M.D., 1995. Forest inventory in Canada with an emphasis on map production. For. Chron. 71 (1), 74–88.

Lehmann, E.A., Wallace, J.F., Caccetta, P.A., Furby, S.L., Zdunic, K., 2012. Forest cover trends from time series Landsat data for the Australian continent. Int. J. Appl. Earth Obs. Geoinf. 21, 453–462.

LePage, P., Banner, A., 2014. Long term recovery of forest sturcture and composition after harvesting in the coastal temperate rainforests of northern British Columbia. For. Ecol. Manag. 318, 250–260.

Madoui, A., Gauthier, S., Leduc, A., Bergeron, Y., Valeria, O., 2015. Monitoring forest recovery following wildfire and harvest in boreal forests using satellite imagery. Forests 6, 4105–4134.

Magnussen, S., Taylor, S.W., 2012. Inter- and intra-annual profiles of fire regimes in the managed forests of Canada and implications for resource sharing. Int. J. Wildland Fire 21, 328–341.

Magnussen, S., Wulder, M.A., 2012. Post-fire canopy height recovery in Canada's boreal forests using airborne laser scanning data. Remote Sens. 4, 1600–1616.

Markham, B.L., Helder, D.L., 2012. Forty-year calibrated record of earth-reflected radiance from Landsat: a review. Remote Sens. Environ. 122, 30–40.

Masek, J.G., Huang, C., Wolfe, R., Cohen, W., Hall, F., Kutler, J., Nelson, P., 2008. North American forest disturbance mapped from a decadal Landsat record. Remote Sens. Environ. 112, 2914–2926.

Masek, J.G., Cohen, W.B., Leckie, D., Wulder, M.A., Vargas, R., de Jong, B., Healey, S., Law, B., Birdsey, R., Houghton, R.A., Mildrexler, D., Goward, S., Smith, W.B., 2011. Recent rates of forest harvest and conversion in North America. J. Geol. Geophys. 116 G00K03. 10.1029/2010JG001471.

McKenney, D., Pedlar, J., Hutchinson, M., Papadopol, P., Lawrence, K., Campbell, K., Milewska, E., Hopkinson, R.F., Price, D., 2013. Spatial climate models for Canada's forestry community. For. Chron. 89, 659–663.

Meigs, G.W., Kennedy, R.E., Cohen, W.B., 2011. A Landsat time series approach to characterize bark beetle and defoliator impacts on tree mortality and surface fuels in conifer forests. Remote Sens. Environ. 115, 3707–3718.

Olofsson, P., Foody, G.M., Herold, M., Stehman, S.V., Woodcock, C.E., Wulder, M.A., 2014. Good practices for estimating area and assessing accuracy of land change. Remote Sens. Environ. 148, 42–57.

Pan, Y., Chen, J.M., Birdsey, R., McCullough, K., He, L., Deng, F., 2010. Age structure and disturbance legacy of North American forests. Biogeosci. Discuss. 7, 979–1020.

Parisien, M.-A., Peters, V.S., Wang, Y., Little, J.M., Bosch, E.M., Stocks, B.J., 2006. Spatial patterns of forest fires in Canada, 1980–1999. Int. J. Wildland Fire 15, 361–374.

Pflugmacher, D., Cohen, W.B., Kennedy, R.E., Yang, Z., 2014. Using Landsat-derived disturbance and recovery history and lidar to map forest biomass dynamics. Remote Sens. Environ. 151, 124–137.

Pickell, P.D., Hermosilla, T., Frazier, R.J., Coops, N.C., Wulder, M.A., 2016. Forest recovery trends derived from Landsat time series for North American boreal forests. Int. J. Remote Sens. 37, 138–149.

Potapov, P.V., Turubanova, S.A., Tyukavina, A., Krylov, A.M., McCarty, J.L., Radeloff, V.C., Hansen, M.C., 2015. Eastern Europe's forest cover dynamics from 1985 to 2012 quantified from the full Landsat archive. Remote Sens. Environ. 159, 28–43.

Schroeder, T.A., Cohen, W.B., Yang, Z., 2007. Patterns of forest regrowth following clearcutting in western Oregon as determined from Landsat time-series. For. Ecol. Manag. 243, 259–273.

Schroeder, T.A., Wulder, M.A., Healey, S.P., Moisen, G.G., 2011. Mapping wildfire and clearcut harvest disturbances in boreal forests with Landsat time series data. Remote Sens. Environ. 115:1421–1433. http://dx.doi.org/10.1016/j.rse.2011.01.022.

Seedre, M., Shrestha, B.M., Chen, H.Y.H., Colombo, S., Jõgiste, K., 2011. Carbon dynamics of North American boreal forest after stand replacing wildfire and clearcut logging. J. For. Res. 16, 168–183.

Seedre, M., Taylor, A.R., Brassard, B.W., Chen, H.Y.H., Jõgiste, K., 2014. Recovery of ecosystem carbon stocks in young boreal forests: a comparison of harvesting and wildfire disturbance. Ecosystems 17, 851–863.

Senf, C., Pflugmacher, D., Wulder, M.A., Hostert, P., 2015. Characterizing spectral–temporal patterns of defoliator and bark beetle disturbances using Landsat time series. Remote Sens. Environ. 170, 166–177.

Slesak, R.A., Kaebisch, T., 2016. Using lidar to assess impacts of forest harvest landings on vegetation height by harvest season and the potential for recovery over time. Can. J. For. Res. 46, 869–875.

Statistics Canada. 2008. *Table 153-0057 - Selected population characteristics, Canada, ecozones and ecoregions with population, every 5 years (number unless otherwise noted)*, CANSIM (Database). Available online (accessed: August 15, 2016): http://www5.statcan.gc.ca/cansim/a26?lang=eng&id=1530057

Stinson, G., Kurz, W.A., Smyth, C.E., Neilson, E.T., Dymond, C.C., Metsaranta, J.M., Boisvenue, C., Rampley, G.J., Li, Q., White, T.M., Blain, D., 2011. An inventory-based analysis of Canada's managed forest carbon dynamics, 1990 to 2008. Glob. Chang. Biol. 17, 2227–2244.

Stocks, B.J., Mason, J.A., Todd, J.B., Bosch, E.M., Wotton, B.M., Amiro, B.D., Flannigan, M.D., Hirsch, K.G., Logan, K.A., Martell, D.L., Skinner, W.R., 2002. Large forest fires in Canada, 1959–1997. J. Geophys. Res. 108, 8149.

Veraverbeke, S., Gitas, I., Katagis, T., Polychronaki, A., Somers, B., Goossens, R., 2012a. Assessing post-fire vegetation recovery using red-near infrared vegetation indices: accounting for background and vegetation variability. ISPRS J. Photogramm. Remote Sens. 68, 28–39.

Veraverbeke, S., Somers, B., Gitas, I., Katagis, T., Polychronaki, A., Goossens, R., 2012b. Spectral mixture analysis to assess post-fire vegetation regeneration using Landsat Thematic Mapper imagery: accounting for soil brightness variation. Int. J. Appl. Earth Obs. Geoinf. 14, 1–11.

Viedma, O., Meliá, J., Segarra, D., García-Haro, J., 1997. Modeling rates of ecosystem recovery after fires by using Landsat TM data. Remote Sens. Environ. 61, 383–398.

Vila, J.P.S., Barbosa, P., 2010. Post-fire vegetation regrowth detection in the Deiva Marina region (Liguria-Italy) using Landsat TM and ETM+ data. Ecol. Model. 221, 75–84.

Vogelmann, J.E., Gallant, A.L., Shi, H., Zhu, Z., 2016. Perspectives on monitoring gradual change across the continuity of Landsat sensors using time-series data. Remote Sens. Environ. 185, 258–270.

White, J.C., Wulder, M.A., Hobart, G.W., Luther, J.E., Hermosilla, T., Griffiths, P., Coops, N.C., Hall, R.J., Hostert, P., Dyk, A., Guindon, L., 2014. Pixel-based image compositing for large-area dense time series applications and science. Can. J. Remote. Sens. 40, 192–212.

Woodcock, C.E., Allen, R.G., Anderson, M., Belward, A., Bindschadler, R., Cohen, W.B., ... Wynne, R., 2008. Free access to Landsat imagery. Science 320 (5879), 1011.

Wulder, M.A., Campbell, C., White, J.C., Flannigan, M., Campbell, I.D., 2007. National circumstances in the international circumboreal community. For. Chron. 83, 539–556.

Wulder, M.A., White, J.C., Cranny, M., Hall, R.J., Luther, J.E., Beaudoin, A., Goodenough, D.G., Dechka, J.A., 2008. Monitoring Canada's forests. Part 1: completion of the EOSD land cover project. Can. J. Remote. Sens. 34, 549–562.

Wulder, M.A., White, J.C., Alvarez, F., Han, T., Rogan, J., Hawkes, B., 2009. Characterizing boreal forest wildfire with multi-temporal Landsat and LiDAR data. Remote Sens. Environ. 113, 1540–1555.

Wulder, M.A., Hilker, T., White, J.C., Coops, N.C., Masek, J.G., Pflugmacher, D., Crevier, Y., 2015. Virtual constellations for global terrestrial monitoring. Remote Sens. Environ. 170, 62–76.

Wulder, M.A., White, J.C., Loveland, T.R., Woodcock, C.E., Belward, A.S., Cohen, W.B., Fosnight, E.A., Shaw, J., Masek, J.G., Roy, D.P., 2016. The Global Landsat Archive: Status, Consolidation, and Direction. Remote Sens. Environ. 185, 271–283.

Zhao, M., Heinsch, F.A., Nemani, R.R., Running, S.W., 2005. Improvements of the MODIS terrestrial gross and net primary production global data set. Remote Sens. Environ. 95 (2), 164–176.

Zhu, Z., Woodcock, C.E., 2014. Automated cloud, cloud shadow, and snow detection inmultitemporal Landsat data: an algorithm designed specifically for monitoring landcover change. Remote Sens. Environ. 152, 217–234.